# The Year of Polar Prediction in the Southern Hemisphere (YOPP-SH)

David H. Bromwich[1], Kirstin Werner[2], Barbara Casati[3], Jordan G. Powers[4], Irina V. Gorodetskaya[5], Francois Massonnet[6],Vito Vitale[7], Victoria J. Heinrich[8], Daniela Liggett[9], Stefanie Arndt[2], Boris Barja[10], Eric Bazile[11], Scott Carpentier[12], Jorge F. Carrasco[10], Taejin Choi[13], Yonghan Choi[13], Steven R. Colwell[14], Raul R. Cordero[15], Massimo Gervasi[16], Thomas Haiden[17], Naohiko Hirasawa[18], Jun Inoue[18], Thomas Jung[2], Heike Kalesse[19], Seong-Joong Kim[13], Matthew A. Lazzara[20], Kevin W. Manning[4], Kimberley Norris[8], Sang-Jong Park[13], Phillip Reid[12], Ignatius Rigor[21], Penny M. Rowe[22], Holger Schmithüsen[2], Patric Seifert[23], Qizhen Sun[24], Taneil Uttal[25], Mario Zannoni[16] and Xun Zou[1].

[1]Byrd Polar and Climate Research Center, Ohio State University, Columbus, OH.

[2]Alfred Wegener Institute Helmholtz Centre for Polar and Marine Research, Bremerhaven, Germany.

[3]Environment and Climate Change Canada, Dorval, Quebec, Canada.

[4]National Center for Atmospheric Research, Boulder, CO.

[5]University of Aveiro, Aveiro, Portugal.

[6]Université catholique de Louvain, Louvain-la-Neuve, Belgium.

[7]Institute of Polar Sciences (CNR-ISP), Bologna, Italy.

[8]University of Tasmania, Hobart, Australia.

[9]University of Canterbury, Christchurch, New Zealand.

[10]University of Magallanes, Punta Arenas, Chile.

[11]National Center for Meteorological Research, Meteo-France, Toulouse, France.

[12]Bureau of Meteorology, Hobart, Australia.

[13]Korea Polar Research Institute, Incheon, Korea.

[14]British Antarctic Survey, Cambridge, United Kingdom.

[15]University of Santiago, Santiago, Chile.

[16]University of Milano Bicocca, Milan, Italy.

[17]European Centre for Medium-Range Weather Forecasts, Reading, United Kingdom.

[18]National Institute of Polar Research, Tokyo, Japan.

[19]Institute for Meteorology, University of Leipzig, Germany.

[20]Space Science and Engineering Center, University of Wisconsin-Madison, Madison, WI.

[21]Polar Science Center, University of Washington, Seattle, WA.

[22]NorthWest Research Associates, Redmond, WA.

[23]Leibniz Institute for Tropospheric Research (TROPOS), Leipzig, Germany.

[24]National Center for Marine Environmental Forecasting, Beijing, China.

[25]Earth Systems Research Laboratory, National Oceanic and Atmospheric Administration, Boulder, CO.

Submitted to *Bulletin of the American Meteorological Society*, February 3, 2020. Revised May 20, 2020.

Corresponding Author: David H Bromwich, Byrd Polar & Climate Research Center, The Ohio State University, Columbus, OH 43210, USA. bromwich.1@osu.edu

**Capulse Summary**

The Year of Polar Prediction in the Southern Hemisphere had a Special Observing Period (SOP) during the 2018-2019 austral summer. Activities during and resulting from the Antarctic SOP are described.

**Abstract**

The Year of Polar Prediction in the Southern Hemisphere (YOPP-SH) had a Special Observing Period (SOP) that ran from November 16, 2018 to February 15, 2019, a period chosen to span the austral warm season months of greatest operational activity in the Antarctic. Some 2200 additional radiosondes were launched during the 3-month SOP, roughly doubling the routine program, and the network of drifting buoys in the Southern Ocean was enhanced. An evaluation of global model forecasts during the SOP and using its data has confirmed that extratropical Southern Hemisphere forecast skill lags behind that in the Northern Hemisphere with the contrast being greatest between the southern and northern polar regions. Reflecting the application of the SOP data, early results from observing system experiments show that the additional radiosondes yield the greatest forecast improvement for deep cyclones near the Antarctic coast. The SOP data have been applied to provide insights on an atmospheric river event during the YOPP-SH SOP that presented a challenging forecast and that impacted southern South America and the Antarctic Peninsula. YOPP-SH data have also been applied in determinations that seasonal predictions by coupled atmosphere-ocean-sea ice models struggle to capture the spatial and temporal characteristics of the Antarctic sea ice minimum. Education, outreach, and communication activities have supported the YOPP-SH SOP efforts. Based on the success of this Antarctic summer YOPP-SH SOP, a winter YOPP-SH SOP is being organized to support explorations of Antarctic atmospheric predictability in the austral cold season when the southern sea-ice cover is rapidly expanding.

## 1. *Introduction*

The Polar Prediction Project (PPP) is a ten-year (2013–2022) initiative of the World Meteorological Organization's (WMO) World Weather Research Programme (WWRP) with the aim of promoting cooperative international research enabling significantly improved weather and environmental prediction services for the polar regions, on time scales from hours to seasonal (Jung et al. 2016). PPP (https://www.polarprediction.net/) is coordinated by the International Coordination Office for Polar Prediction (ICO) hosted by the German Alfred Wegener Institute Helmholtz Centre for Polar and Marine Research.

As a flagship activity of PPP, the Year of Polar Prediction (YOPP) was launched in May 2017. By coordinating a period of intensive observing, modeling, verification, user-engagement and education activities, YOPP seeks to enable a significant improvement in environmental prediction capabilities for the polar regions and beyond. From mid-2017 to mid-2019, during three YOPP Special Observing Periods (SOP) in the Arctic and Antarctic routine observations, such as radiosonde launches and deployments of buoys, were enhanced. These extra data feed into numerical weather prediction (NWP) experiments to allow study of the benefits of additional data to advance predictive skills of polar weather and sea-ice conditions. The European Centre for Medium-Range Weather Forecasts (ECMWF) provides an archive of their twice daily global coupled atmosphere-ocean-sea ice-land model forecasts for the entire YOPP period starting in May 2017 – see the YOPP Data Portal (https://yopp.met.no/) for details.

This paper offers an overview of the key activities associated with efforts during YOPP in the Southern Hemisphere, some of the main findings obtained so far, and plans for the future.

## 2. *Summer Special Observing Period*

The YOPP-SOP in the Southern Hemisphere ran from November 16, 2018 to February 15, 2019 to span the period of greatest operational activity during austral summer in the Antarctic. The primary additional observations were radiosonde ascents and drifting buoy deployments, plans for which were developed during three international workshops. Figure 1 shows that 2,244 additional radiosondes were launched during the SOP from 24 land-based stations and 5 ships (plotted in nominal locations); King George Island and Terra Nova Bay each amalgamate two adjacent stations. Seventeen nations contributed to the greatly enhanced continental coverage that varied by location from a few additional soundings over limited periods to sustained efforts throughout the SOP to increase the coverage up to four times per day at Neumayer III station and Terra Nova Bay. During the SOP an average of 24 additional radiosondes were launched each day, roughly doubling the number of routine soundings, but this increase was not uniform in time. Most soundings were transmitted to the WMO Global Telecommunications System (GTS) for real-time use by global forecasting centers. Monitoring of SOP radiosonde reports received in National Centers for Environmental Prediction (NCEP) data streams was conducted by AMPS (see below, http://www2.mmm.ucar.edu/rt/amps/status/prepbufr_raob_accounting.html). An open-access archive of the additional SOP soundings plus some regularly scheduled ascents was established by British Antarctic Survey (ftp://ftp.bas.ac.uk/src/YOPP-SH/radiosondes/). This unique data set is the foundation for the observing system experiments summarized in section 4.

Of all the meteorological observational networks across the Antarctic, the surface network consisting of staffed stations and the international automatic weather stations (AWS) is the largest contributor to the routine data collected during YOPP-SH SOP. While there are approximately 30 staffed stations, there are over 160 AWS units installed and operating across the continent (Figure 2). Several YOPP-endorsed projects (see for details on YOPP endorsement at https://www.polarprediction.net/key-yopp-activities/yopp-endorsement/) contributed to enhanced data collection on various atmospheric and oceanic properties (e.g., CAALC at King George Island, DACAPO-PESO in Punta Arenas). Gonzalez et al. (2019) describe a novel approach for providing additional surface observations for the high Antarctic interior during the SOP using a mobile AWS on a wind-powered sled.

Sea ice and snow are key variables in the global climate system. Through their numerous interactions with the atmosphere (e.g., the ice-albedo feedback) and the ocean (e.g., freshwater budgets during melt and formation), they have strong impacts on global circulation patterns extending far beyond the polar regions. However, the investigation of physical sea-ice and snow parameters during work on one ice floe can only give a snapshot of the sea-ice conditions. To obtain information about the seasonal and interannual variability and evolution of the observed ice floes, autonomous ice tethered platforms (buoys) were deployed measuring the sea ice and snow characteristics before, during and after the SOP. Different kinds of buoys were used: Ice Mass Balance buoys (IMBs) deriving the sea-ice growth; snow-depth buoys (Snow Buoys) measuring the snow accumulation over the course of the year; Surface Velocity Profilers (SVPs) providing information on the local oceanic and sea-ice drift; radiation stations measuring spectral incoming, reflected and transmitted shortwave radiation fluxes; salinity and optical harps measuring *in-situ* vertical profiles of salt, solid fraction, temperature and light during sea-ice growth and decline. In addition, buoys are partly equipped with sensors measuring air and/or body temperature and sea level pressure. All SVP and Snow Buoys report their position together with measurements of surface temperature and atmospheric pressure directly into the GTS for use by the global forecasting centers. Figure 3 gives an overview of all buoys that were active near the start of the YOPP-SH SOP in November 2018. All buoys that were deployed and have been active in Antarctica can be viewed at the website http://iabp.apl.washington.edu/IPAB_Table.html provided by the International Programme for Antarctic Buoys (IPAB).

During the YOPP-SH SOP, 13 buoys deployed by the Alfred Wegener Institute in preparation for the SOP were active in the Weddell Sea (Figure 4). These can be categorized in chronological order as follows:

1. At the German overwintering station Neumayer, one Snow Buoy has been installed since 2013 for reference measurements which therefore also contributed to the YOPP-SH SOP.
2. During the PS96 expedition from December 2015 to February 2016 with the German icebreaker RV Polarstern, a large number of buoys were deployed on the ice. One of the buoys entered the Antarctic Circumpolar Current and circumnavigated the entire Antarctic. This buoy was also active during YOPP-SH SOP and at that time was west of the Antarctic Peninsula.
3. During the PS111 expedition from January to March 2018 a large number of buoys of all kinds were deployed on the ice. Of these, two Snow Buoys, one IMB and one radiation station were still active during the SOP while drifting on pack ice through the Weddell Sea.
4. On the fast ice in Atka Bay near Neumayer station, one Snow Buoy and one IMB were installed on the ice during austral winter 2018. Both buoys were still active during the SOP and located in Atka Bay.
5. During the “Weddell Sea Expedition 2019” several SVPs were deployed in the northern and western Weddell Sea with the South African icebreaker Agulhas II. Five of them were

active during the SOP and were placed on the ice between January 16 and February 13, 2019.

### 3. *Performance of Global Numerical Weather Prediction (NWP) Models*

The performance of several operational global models over Antarctica was contrasted to their performance over lower latitudes during the YOPP-SH SOP using the anomaly correlation, which spatially compares the forecast anomalies with those observed, as a function of forecast day. The models imported observations from the GTS including extra SOP radiosondes, so it is not possible to determine their forecast impact from this anomaly correlation analysis. The top panel of Figure 5 shows that the 500-hPa geopotential height anomaly correlation coefficient for Antarctica is 12 to 18 hours poorer than that for the extratropical Southern Hemisphere (all latitudes poleward of 20ºS) after day 4; this is seen by comparing the dashed lines with the solid lines for each color (model). The bottom panel of Figure 5 illustrates, for comparison, that the anomaly correlation coefficient over the Arctic is only 0 to 6 hours behind that for the extratropical Northern Hemisphere (all latitudes poleward of 20ºN). Figure 5 demonstrates that the contrast in summer predictability of the polar regions versus mid-latitudes is larger for the Southern Hemisphere than for the Northern Hemisphere. Presumably this poorer predictability for the Antarctic compared to the extratropical hemisphere arises because of the much more limited observational coverage and incomplete understanding of the atmospheric processes, implying that YOPP-SH SOP efforts can result in significant forecast improvements.

In addition to the multi-model results, two models were assessed in more detail: the Global Deterministic Prediction System (GDPS) and ARPEGE-SH (see below). Environment and Climate Change Canada (ECCC) examined its GDPS over Antarctica during the summer SOP, and found: better performance of the surface variables for the forecasts initiated at 12

UTC, rather than 00 UTC (not shown); a strong diurnal cycle and a systematic cold bias of surface air temperature (Figure 6), which is partially due to an over-prediction of clear sky and under-prediction of cloudy conditions (not shown); and a systematic under-estimation of strong winds, whereas weak winds (often associated with night inversions) are overestimated (not shown). These latter characteristics of the wind speed bias, as well as the diurnal cycle of the temperature bias, are systematic errors that are found globally, common also to other models, whereas the better performance at 12 UTC is atypical, and in the Northern Hemisphere usually 00 UTC runs perform the best.

Using the ECCC-GDPS, the YOPP verification exercise has provided the opportunity to test some of the new WMO recommendations for evaluation of surface variable forecasts (WMO-485, Appendix 2.2.34), and how these might be improved and/or adapted, accounting for the particular environmental conditions of the polar regions. Figure 6 shows the ECCC-GDPS surface air temperature bias evaluated for the raw model output (red lines), and for the model output adjusted to the station elevation by applying a constant WMO-recommended lapse rate (0.0065 ºC/m, gray lines) and the dry-adiabatic lapse rate (0.0098 ºC/m, blue lines). The cold bias is improved when applying the WMO-recommended standard-atmosphere lapse rate adjustment, and it further improves when applying the dry-adiabatic lapse rate, which better represents the characteristics of the Antarctic summer vertical temperature profile. The bias systematically improves as well when calculated excluding stations which differ in elevation by more than 500m from the model-tile altitude (dashed lines), suggesting that the lapse-rate adjustment should be performed solely for small elevation corrections.

In support of the YOPP-SH effort, Météo-France created a specific model configuration for the YOPP-SH SOP called ARPEGE-SH. It is based on the ARPEGE global model used for numerical weather prediction (Pailleux et al. 2015, used in Figure 5) but with the high resolution area (~ 7.5 km) relocated over Antarctica instead of over France. A 4DVAR assimilation was performed every 6h with the observations used by the ARPEGE operational version. 10-day and 5-day forecasts have been produced at 00UTC and 12UTC respectively. The added value (blue lines) of this configuration thanks to the increase of the horizontal resolution of ARPEGE-SH can be seen in Figure 7 for the temperature compared to the radiosoundings and the ERA5 global reanalysis. Another factor that may have contributed to the better forecast performance of ARPEGE-SH is an increase of the number of assimilated radiosonde temperature observations used in the boundary layer, 176 more for a total of 680 for the entire YOPP-SH SOP.

## *4. Preliminary Results from Observing System Experiments*

### *4.1 The Antarctic Mesoscale Prediction System (AMPS)*

AMPS is a real-time NWP system with a primary mission of providing model guidance to the forecasters of the U.S. Antarctic Program (Powers et al. 2012). AMPS also supports researchers, international Antarctic efforts, and scientific field campaigns, and its forecasts are freely available via http://www2.mmm.ucar.edu/rt/amps. AMPS is run by the National Center for Atmospheric Research (NCAR), and it features the Weather Research and Forecasting (WRF) Model (Skamarock et al. 2019). Figure 8 shows the WRF domains, having horizontal grid spacings of 24 km (Southern Ocean), 8 km (Antarctica), 2.67 km (Ross Ice Shelf, Antarctic Peninsula), and 0.89 km (Ross Island region).

In a targeted study the AMPS framework and WRF are being applied to understand the forecast impact of the additional YOPP-SH SOP radiosonde data. WRF simulation experiments assimilate the extra soundings of the SOP using two methodologies: one varying the data assimilated and one varying the data assimilation (DA) procedure. For the former, a control configuration has WRF forecasts assimilating the set of routine (i.e., pre-SOP) observations available to AMPS ("no-SOP" runs), while the test configuration adds the extra SOP soundings to that observation set ("SOP" runs) in the assimilation step.[1] The second methodology varies the techniques for generating the background error (BE) covariance input to the DA system used for forecast initialization. That system, WRFDA (Barker et al. 2012), employs a hybrid 3-dimensional ensemble/variational approach (3DEnVar) (Wang et al. 2008). Preliminary results are presented here of WRF forecasts for a significant weather case of the strongest low in the Amundsen Sea off Marie Byrd Land during the December 28, 2018-January 20, 2019 test period. For initial evaluation only the 24-km AMPS WRF domain (Figure 8) was run.

There is a clear forecast improvement from the additional SOP soundings in forecasting the target cyclone. Figure 9 shows this via comparisons of SOP and no-SOP 48-hr forecasts of sea level pressure and surface winds with the ERA5 global reanalysis. The low center and its orientation along with the surface wind field are better captured in the SOP run, as is the blocking anticyclone at 300 hPa that steered the surface low more toward the coast (not shown). Figure 10 compares observed time series of surface pressure, temperature, and wind speed from Austin AWS, located in West Antarctica (position marked in Figure 9), with the experiment forecasts and the ERA5 global reanalysis. All other coastal AWS in this region had large amounts of missing observations and no wind speed measurements. The surface pressure forecast is better for the SOP run (top panel, red curve) than the no-SOP run (blue curve), with

[1] The routine observations used in AMPS are: surface data (e.g., AWS, SYNOP, METAR); upper-air soundings; aircraft observations; ship and buoy observations; geostationary and polar-orbiting satellite AMVs (atmospheric motion vectors); GPS radio occultations; and AMSU (Advanced Microwave Sounding Unit) radiances.

the former bias being 2.8 hPa compared to the latter of 4.6 hPa. Similarly, the SOP run's wind speed forecast (bottom panel) is closer to the observations, with the SOP wind speed bias less than that of no-SOP (1.3 $ms^{-1}$ v. -3.3 $ms^{-1}$). The positive impact on predictive skill of the SOP soundings is consistent with the recent findings of Sato et al. (2020) who reported that the assimilation of data from just two additional radiosonde sites in East Antarctica improved forecast performance for a strong Antarctic cyclone event near Syowa station (see next section).

### *4.2 Extreme weather events*

Prior to the YOPP-SH SOP, a Japanese research group preliminarily investigated the impacts of additional radiosonde observations in the Antarctic on predicting storms in high and midlatitudes in the Southern Hemisphere. They used an atmospheric general circulation model, AFES (~1° × 1° and 48 vertical levels) (Enomoto et al. 2008, Ohfuchi et al. 2004) with 63 ensemble members. The DA system ALEDAS2 (Enomoto et al. 2013) consists of the AFES and a local ensemble transform Kalman filter (LETKF, Hunt et al. 2007, Miyoshi and Yamane 2007). Similar efforts in the Northern Hemisphere found that the flow-dependent observational signal trapped in a tropospheric potential vorticity is a fundamental factor for understanding the improved forecast skill of both of winter and summer storms on the time scale of 3 to 5 forecast days (Inoue et al. 2015, Yamazaki et al. 2015, Sato et al. 2017, 2018a).

Two storm cases in the Southern Hemisphere were investigated prior to YOPP-SH SOP. The first case was a midlatitude cyclone over Tasmania which caused heavy precipitation and snowfall over the island on 3 December 2017. From 29 October 2017 to 4 December 2017, extra radiosonde observations were launched over the Southern Ocean from the Australian RV Aurora Australis (Sato et al. 2018b). The other case is a strong cyclone event which caused unusually strong winds at the Japanese station Syowa (69.00°S, 39.58°E) in early January 2018 (Sato et al.

2020). From late December 2017 to early January 2018, extra radiosonde observations were made at the Japanese Antarctic station Dome Fuji (77.8°S, 39.1°E) at 12 and 18 UTC. In both cases, two initial fields, one that included the extra observations and the other that excluded them, were prepared by using ALEDAS2. The successful ensemble prediction for each case of cyclone development and trajectory only occurred in the experiment that included the additional radiosonde observations. Downstream propagation of these observational signals remotely influenced the predictability of a midlatitude cyclone over the Tasman Sea and a cyclone along the Antarctic coast. The difference in ensemble spread at upper levels is one way to track the observational signals. These results demonstrate that extra observations for a sparse observing network such as the Southern Ocean and the inner Antarctic ice sheet potentially can improve the forecast skill of mid-latitude and polar weather phenomena in the Southern Hemisphere.

Although satellite data improve upper tropospheric fields, results from YOPP efforts in the Northern Hemisphere show that a skillful forecast of atmospheric circulation in the mid and lower troposphere still depends on radiosondes (Day et al. 2020). The role of extra radiosondes on weather predictions in the Antarctic and mid-latitudes of the Southern Hemisphere will be further investigated by focusing on the contrast of observing networks between the Antarctic and Arctic.

### *5. Atmospheric Rivers*

Atmospheric rivers (ARs) impact Antarctic surface mass balance through transport of anomalous heat and moisture from subtropical regions. Antarctic ARs have been linked to extreme precipitation events (Gorodetskaya et al 2014), a temperature record (Bozkurt et al 2018) and surface melt events (Wille et al 2019). Using frequent YOPP-SH SOP and regular radiosonde observations at Neumayer and Syowa stations, Gorodetskaya et al (2020) showed that extremes in lower tropospheric humidity, temperature, wind speed, and moisture transport are associated with ARs, and are not always well represented by reanalysis products. Here we present a special AR case affecting simultaneously the southern extreme of South America and the Antarctic Peninsula, which we characterize using YOPP-SH SOP observations from both continents. On the Antarctic Peninsula, the surface mass balance can be especially sensitive to AR events during summer, when surface temperatures vary around zero and frequent transitions occur between snow and rainfall.

On 6 December 2018, a corridor of anomalous moisture began at the subtropical southern Pacific, extended through the southern extreme of South America, and terminated at the Antarctic Peninsula (Figure 11a). This AR was associated with a deep cyclone in the Bellingshausen Sea and a vast high-pressure system over the South American continent, stretching to the eastern part of the Weddell Sea (Figure 11a). Measurements made within the scope of YOPP-SH SOP, such as CAALC on King George Island (KGI) near the northern Antarctic Peninsula and DACAPO-PESO at Punta Arenas (southern Chile), allow for a detailed characterization of the temporal evolution of this AR event and its impacts.

At Punta Arenas, the integrated water vapor (IWV) retrieved from a microwave radiometer almost doubled on 6 December from 0 to 11 UTC (17 kg $m^{-2}$ to 31 kg $m^{-2}$) and stayed elevated until 18 UTC (Figure 11b, blue). A radiosounding at 12 UTC confirmed the elevated IWV amount (27.8 kg $m^{-2}$, not shown). Cloud radar observations showed that from 0 to 12 UTC midlevel and deep clouds persisted, with tops ranging from 6 to 12 km and a 0°C level melting layer height of ~3 km agl (from 3 UTC onward). Liquid-containing clouds of varying geometrical thickness were observed, with liquid water path (LWP) peaking at ~1.7 kg/$m^2$ at 11 UTC, followed by lower clouds with smaller LWPs (Figure 11b, black). Light rainfall was observed at elevated heights but mostly evaporated before reaching the surface. The lack of moisture loss via precipitation when the AR was passing over the southern extreme of South America allowed the enhanced IWV to reach and strongly affect Antarctic Peninsula weather and surface radiation.

At KGI, the radiosonde-derived IWV for the entire profile also peaked on 6 December at 11 UTC (17 kg $m^{-2}$; Figure 11b, red dots) and the integrated vapor transport reached 422 kg $m^{-1}$ $s^{-1}$. Vertical profiles reveal horizontal moisture transport of up to 120 g $kg^{-1}$ m $s^{-1}$ at ~800 hPa, driven by specific humidity in excess of 4 g $kg^{-1}$ and strong winds (Figure 11c). In the lower troposphere, both zonal and meridional components contributed to the total (Figure 11c). The AR event at KGI was characterized by warming of the boundary layer with continuous moisture advection; persistent thick, low-level liquid clouds; and strong influences on the surface radiation budget (Figure 11d). The low, thick liquid-containing clouds enhanced downwelling longwave radiation (by ~100 W/$m^2$), but during the daytime this was more than offset by strong attenuation of shortwave radiation by clouds (Figure 11d). Comparing measured and (simulated) clear-sky radiation indicates that cloud forcing was strongly positive at night and negative during the day. Precipitation changed from snowfall on 5 December to rain and mixed-phase precipitation on 6 December.

These conditions have important consequences for air, ship and station operations around the Antarctic Peninsula. However, regional climate and weather prediction models struggle to correctly forecast weather conditions during AR events. To assess this challenge, as well as the importance of local-scale prediction, comparisons were made between WRF model runs with and without radiosoundings made at King Sejong station on KGI. In this experiment, the data assimilation (DA) run incorporates the radiosoundings, and is contrasted with the control (CTL) run without the radiosoundings, as well as with the ERA5 global reanalysis. Compared to the DA run, the CTL run had small differences in temperature forecasts (not shown) and more significant differences in wind speed (Figure 11e, right top). Both CTL and DA runs capture strong wind periods (with peaks exceeding 15 m $s^{-1}$) at 0612 and 0718 UTC, but with some overestimation. Compared to station measurements, the DA run slightly improved the rainfall forecast, with larger values in better agreement, but still underestimated the peak in precipitation (Figure 11e, right bottom). KGI received only moderate amounts of precipitation compared to the western side of the Antarctic Peninsula, where the difference between the observed and modeled values could be much larger (Figure 11e, left).

## *6. SIPN South*

After 35 years of modest expansion, Antarctic sea-ice extent has declined dramatically since 2015 (Parkinson 2019). The recent negative sea-ice extent anomalies, which peaked in 2016, have been interpreted in turn as an extra-tropical response to the major El-Niño event during the boreal winter 2015-2016, enhanced by record-low levels of the Southern Annular Mode (SAM) in late 2016 (Stuecker et al. 2017), as the result of anomalous southward oceanic advection in winter and early spring 2016 (Schlosser et al. 2018), and as a consequence of prolonged warmer conditions in the upper ocean (Meehl et al. 2019). Dynamic forcing by winds on sea ice was also proposed as a possible cause for the sudden sea-ice retreat (Wang et al. 2019).

This case illustrates that our understanding of Antarctic sea-ice variability, including its drivers, is far from complete – and certainly less advanced than in the Arctic. A corollary is that our understanding of Antarctic sea-ice *predictability* remains limited, too. However, recent studies (Holland et al. 2013, 2017, Ordoñez et al. 2018, Marchi et al. 2019) have highlighted several physical predictability mechanisms that suggest potential prediction skill extending for at least a season. It remains to be demonstrated whether these mechanisms can be translated into actual prediction skill (Zampieri et al. 2019).

The Sea Ice Prediction Network South (SIPN South) was established in 2017 with the triple goal of: (i) identifying existing institutional efforts in terms of seasonal Southern Ocean sea-ice forecasting; (ii) producing the first-ever coordinated experiment to benchmark predictions against a common forecasting target; and (iii) documenting the levels of skill of contemporary prediction systems. The ultimate scientific objective of SIPN South is to understand the causes of forecast errors and guide the development of forecasting systems.

YOPP endorsed SIPN South in 2017. Over the course of two years (2017-2019), SIPN South collected 358 forecasts issued by 16 unique groups or individuals, representing five continents. The requirement for participation in SIPN South is to be able to provide daily estimates of circumpolar (total) Antarctic sea-ice area for the target period December to February. Most contributors also provided regional information. The method of forecasting is left to the discretion of contributors; the pool of forecasts currently consists of dynamical model contributions (generated from ocean-sea ice or fully coupled climate models) and statistical contributions (based on empirical statistical models trained on past observed data). All forecasts received so far are hosted in an open-access database (https://github.com/fmassonn/sipn-south-public).

The analyses conducted up to now, based on two coordinated forecasts (austral summer 2017-2018 and 2018-2019), have led to four main conclusions. *First,* the circumpolar total Antarctic sea-ice area is generally well forecast, and no obvious systematic bias can be detected for that diagnostic. However, this apparent agreement masks strong regional differences. For example, sea-ice area was overestimated in the Ross Sea in February 2018 in all contributions but one. *Second*, the timing of the minimum of Antarctic sea-ice area is not predicted well by the forecasts. While the date of the minimum is not expected to be predicted exactly (because it is influenced by synoptic conditions that forecasting systems cannot anticipate a few months in advance), ensembles should reflect this weather uncertainty and encompass the observed timing of minimum. This is not the case even for contributions producing large ensembles. *Third*, dynamical models experience issues with initialization: in several model-based contributions, sea ice is biased high from the first day of the integration. This problem illustrates the challenges in assimilating sea-ice concentration while preserving the physical consistency with the ocean in the models. *Fourth*, based on the most recent forecasting exercise (austral summer 2018-2019), statistical contributions appear to be superior to dynamical model contributions in terms of the spatial representation of sea-ice concentration (Figure 12). The robustness of this result has yet to be confirmed. A possible explanation might be that dynamical models are superior to statistical ones when very anomalous summer conditions occur. Massonnet et al. (2018, 2019) provide further details and analyses of the results of the coordinated experiments.

## *7. YOPPsiteMIP in the Antarctic*

The PPP Steering Group has initiated a coordinated process-based model evaluation using high-frequency multi-variate observations at selected Arctic and Antarctic supersites, during YOPP. The aim of this YOPP site Model Intercomparison Project (YOPPsiteMIP) is to deepen our understanding on the representation of current environmental prediction systems of polar processes, both in the atmosphere, land, sea-ice or ocean components, and in the coupling at their interfaces.

The Antarctic sites and supersites are Alexander Tall Tower AWS, Casey, Davis, Dome Concordia, Dumont D'Urville, Halley IV, Jang Bogo, King George Island, Georg Von Neumayer, Mawson, Syowa, Amundsen-Scott South Pole, Byrd, Rothera, Vostok, McMurdo, and Troll (Figure 1 shows most of these locations). These sites span the diversity in climatology and topography found in Antarctica and thus represent a variety of challenges for NWP systems. Some of these sites host multiple systems deployed for long-term monitoring, and suites of instruments that provide detailed measurements characterizing the vertical column of the atmosphere as well as the surface conditions and energy fluxes. This offers a good setting for polar process evaluation.

In support of YOPPsiteMIP, several international modeling centers (such as Météo-France, ECMWF and ECCC) are providing NWP time series at high frequency (on the order of model time-step) and on model levels, in correspondence of the super-site locations, for physical variables supported by the observations at the sites. This unique dataset of paired model output and multi-variate high-frequency observations enables process-based analysis investigating topics such as the representation of hydrometeors and cloud microphysics; low level clouds; stable boundary layer;  radiation, turbulence and energy budgets; energy and momentum fluxes; coupling between ocean-cryosphere–atmosphere; and atmosphere–snow interaction.

The Antarctic YOPPsiteMIP dataset is open-access and intended to be made widely available through the YOPP Data Portal for the benefit of the global scientific community and operational forecasting centers. ECMWF and ARPEGE model time series are already available at https://thredds.met.no/thredds/catalog/alertness/YOPP_supersite/catalog.html. YOPPsiteMIP is a project in evolution (http://www.polarprediction.net/yopp-activities/YOPPsiteMIP) that encourages the contribution by other modeling centers and welcomes evaluation studies.

## *8. Education, Outreach and Communication Activities.*

### *8.1 CAPIRE-YOPP*

From October 2018 to June 2019, the Italian educational project entitled *Comprendere lA PrevIsione meteoRologica in antartidE sostenendo YOPP* (CAPIRE-YOPP) involved 17 classes from 7 intermediate and high-schools (about 350 students) from the Milan region in a set of activities connected to polar meteorology and climate (Figure 13).

Following the overarching idea of making a concrete connection with Italian researchers participating in the YOPP-SH SOP in Antarctica, the project supported the launch of about 30 extra radiosondes from the Italian-French plateau station, Dome Concordia. From 1 to 15 January 2019, Concordia station for the first time performed four daily radiosoundings at synoptic hours 00, 06, 12 and 18 UTC. The unique data set produced during these two weeks in January added to the 4 soundings per day released from Terra Nova Bay on the Antarctic coast from a joint Italian-Korean collaboration.

Field activities and data collected in Antarctica provided a strong base to build a wide-ranging educational activity. The project aimed to include students of different ages and actively involved teachers to develop tools to connect students with the YOPP topics. Activities included in-depth events, seminars, lessons and a visit to the operational meteorological center of Milan Linate airport. Field activities in Antarctica related to the project offered a variety of student activities, as described below.

Students were given the opportunity to meet remotely with researchers involved in the SOP. Remote connections with Antarctica were made on two occasions: on 27 November 2018, a live connection via Internet with the Italian Antarctic Mario Zucchelli station allowed students and teachers to talk with scientists carrying out meteorological observations; and on 14 January 2019, the final day of field work devoted to CAPIRE-YOPP, another live connection with the Italian-

French Antarctic station Concordia gave a delegation of students and professors the opportunity to meet the researchers engaged with the extra radiosonde releases during the SOP.

Younger students were also kept actively engaged through the following activities: (i) composing short poems on meteorology/clouds, (ii) creating artistic (e.g., dioramas) or technical (orthogonal projections) products, and (iii) producing multi-media products. The best student drawings were attached to weather balloons released from Concordia station, personalizing radiosonde launches. High-school students were involved in performing data analysis and the presentation of their scientific results.

Each of the educational activities was characterized by friendly competition, in order to stimulate engagement and interest. For each activity category, outputs were evaluated by the researchers involved in the project and by teachers. In the spirit of cooperation and fairness, attention has been paid to distribute winners among classes. Winner findings were presented at a final event organized at the University of Milan in June 2019. In addition to awards for contest winners, all classes, teachers and experts engaged in activities received certificates of attendance as a memento of their participation.

Thanks to CAPIRE-YOPP, students were provided with a unique opportunity to learn and apply scientific methods and techniques, and become familiar with the language of scientific research, and topics related to polar meteorology.

### *8.2 Weather Information Usage*

People in Antarctica and the sub-Antarctic make weather-related decisions every day, from simply deciding “is it safe to go outside?”, to the complex programming of flights and scientific projects, such as determining the weather window (weather conditions suitable for a task) occurring: is it long enough to complete the task(s)?; how quickly will I become cold or frostbitten? If a blizzard is expected one would not want to start a long maintenance job outside, or scientific data collection that relies on calm conditions. In harsh environments, isolated locations, or time-poor situations, good decision-making, trust in and reliance on weather information, and understanding the uncertainties in a forecast or weather model are vital for safe operations and human survival in the Antarctic. "*Understanding the use of forecast information in decision-making*" is a high-priority WMO WWRP research theme (Morss et al. 2008) and important within the PPP (Dawson et al. 2017). Yet, there is little evidence-based research available to support best practice decision-making to improve human health, safety and performance in the Antarctic context.

A doctoral research project undertaken by Victoria Heinrich at the University of Tasmania addresses some of these shortfalls, applying psychological theory to examine how, when, and why people use weather and climate information, and how comprehension, relevance, and use of this information might be improved. The current study involves participants (recruited until April 2020) who have recently been deployed to the Antarctic and/ or sub-Antarctic. An online questionnaire and semi-structured qualitative interviews collected background information on the type and context of people's weather-related decisions, their weather information sources and preferences, work environment, and risk perception. Data and themes from this study will provide an overview of Antarctic weather decision-making, the demands, pressures, constraints, and needs of the users, and will inform later stages of the project. Early results suggest the most useful information are wind direction and speed, weather information/advice from trained weather professionals, and weather forecasts (see Figure 14). The next study will use a series of experiments to examine factors that influence the quality of individual's decision-making including experience, weather salience, time pressures, conflicting goals, biases, and heuristics.

*8.3. Communication and Social Media Engagement*

Communication within PPP is important to facilitate engagement of the polar prediction community, i.e., scientists, experts from NWP centers, and various users of available polar forecast services and products. While stakeholder engagement within academia still has specific challenges, social media platforms make it possible to reach out to a greater number of stakeholder groups. The @polarprediction social media platforms on Twitter and Instagram are important instruments for PPP to (i) inform about current developments and activities and (ii) motivate stakeholders to engage with PPP/YOPP. In this regard, (internal) communication to the involved scientists, forecast providers and forecast users cannot be considered separate from the (external) communication to the wider interested polar prediction community. Furthermore, successfully conducted external communication that is prepared particularly for non-experts has been shown to increase engagement among the wider community while at the same time enhancing active participation among the already-engaged community members (Werner 2017).

In order to prepare for communication activities during YOPP-SH SOP, YOPP-endorsed projects and forecasting centers that committed contributions to YOPP-SH SOP were asked to either actively use their social media platforms and mention @polarprediction, or send photo and video material including respective copyright information to the YOPP Coordination Office for use on social media and the PPP website www.polarprediction.net. Figure 15 shows website, social media and email list engagement during YOPP-SH SOP. The data indicate active engagement of the science community (e.g., @Antarctica.cl) and the weather forecast providers (e.g., @MeteoFrance, @AEMET_antartida, @antarctica.gov.au, @TROPOS_eu) with

YOPP/PPP. In particular, scientists involved in YOPP-endorsed projects who ran their own social media account actively followed and engaged with @polarprediction.

## *9. Further Plans for YOPP-SH*

### *9.1 Consolidation Phase.*

In July 2019, PPP moved from the YOPP Core Phase into its Consolidation Phase (Figure 16). During the final three years of PPP (until the end of 2022), the data collected during the core phase will be made available to the community (see YOPP Data Portal) to improve predictive models and eventually transform these into more reliable products for people living and working in polar regions. While cutting-edge science activities will also underpin the Consolidation Phase, including a YOPP Targeted Observing Period aligned with the MOSAiC ice drift (https://www.mosaic-expedition.org/) and a YOPP SOP during Antarctic winter 2022 (see below), the focus of the three final years of PPP will be on the translation of scientific insights gained during the YOPP Core Phase into advanced and more reliable weather and sea-ice forecast services. In addition to consolidating and synthesising YOPP research and science, it will be necessary to prepare the ground for a post-YOPP structure of coordination and communication. To provide guidelines and structures on how to realize these goals, a third version of the YOPP Implementation Plan has been published in early 2020 (https://www.polarprediction.net/about/implementation-and-science-plans/). This document updates two previous versions of the plan, giving detailed descriptions of actions during the YOPP Consolidation Phase, including strategies and objectives in light of the results achieved until now.

### *9.2 YOPP-SH Activities during the Consolidation Phase*

The activities initiated in conjunction with summer YOPP-SH SOP (described above) will be brought to fruition during the PPP Consolidation Phase. Enhanced physical parameterizations to correct known model biases and ensemble data assimilation will be implemented into AMPS with the goal of substantially improving the forecast skill. More generally, the YOPPsiteMIP activity will lead to better understanding and improvement of Antarctic model physics for participants, especially for the international forecasting centers. SIPN South is continuing to provide baseline performance evaluation of coupled model forecasts of summer season sea-ice behaviour around Antarctica and a dedicated experiment for the winter 2022 SOP is envisaged. Future investigations will delve into the causes of the wide range of forecast behaviour exhibited. Observing system experiments are being conducted by several groups to better identify the added value of the enhanced summer SOP observations and to provide guidance for an expanded Antarctic observational network.

At the 4$^{th}$ Workshop on YOPP-SH held in Charleston, South Carolina during June 2019, it was recognized there is a compelling interest to extend the operational season beyond the austral summer to fall and early winter. From a scientific perspective, the active weather conditions at that time are expected to be more challenging to forecast than the generally benign summer, and the sea-ice cover is rapidly expanding. It was decided to hold a second YOPP-SH SOP scheduled for mid-April to mid-July 2022 to sample the non-summer conditions. In view of the emerging appreciation that the greatest forecast impact of additional in-situ observations occurs in conjunction with major cyclone events, the enhanced data collection will be targeted for those occasions (i.e., Targeted Observing Periods), and particular regions like the Ross Sea vicinity will be emphasized. This approach also recognizes that personnel numbers are much smaller at this time of year, making sustained circumpolar observing during a 3-month SOP impractical. The physical oceanographic community will be engaged to explore the coupling between the atmosphere and ocean during sea-ice growth and its role in the evolution of Southern Ocean cyclones to determine how well these phenomena are represented in forecast models.

During the Consolidation Phase, aspects of stakeholder engagement in relation to the YOPP-SH will continue to be developed via a Special Services Period, discussed next.

*9.3 Special Services Period*

During the Special Services Period, the current status, value and impact of polar environmental forecasting services and endeavor to aid in the transition of science into services will be assessed. To achieve such a set of ambitious goals, a series of targeted and facilitated focus-group discussions between researchers involved in YOPP-SH and forecasting service providers and users are required. A one-day Antarctic Weather & Society Workshop was originally scheduled to be held on 1 August 2020 in conjunction with the Workshop on Antarctic Meteorology and Climate (WAMC) and on the margins of the Scientific Committee on Antarctic Research's Open Science Conference (SCAR OSC) in Hobart, Tasmania. However, as a result of travel restrictions and logistic uncertainties arising from the Covid-19 pandemic, both the WAMC and the SCAR OSC have been cancelled. Consequently, the planned Antarctic Weather & Society Workshop will now be held in conjunction with the next WAMC, which is scheduled for June 7-9, 2021 at the Byrd Polar and Climate Research Center in Columbus, Ohio.

Addressing the overarching research question "How do we ensure that society benefits through applications of better weather programs and information services in the Polar regions?", this Weather & Society Workshop aims to: (i) create dialogue between environmental forecasters, researchers and end-users of environmental forecasts for the Antarctic region; (ii) understand the role and relevance of environmental forecasting services in decision-making processes during Antarctic operations; and (iii) engage and learn from users and providers regarding how best to present Antarctic environmental forecasts.

The workshop will employ a series of participatory and interactive focus-group discussions using a world-café format. Background information on the PPP and YOPP-SH, as well as a small survey, will be shared with invited participants before the workshop, with the results of the survey being presented and built on during the workshop. To understand the role and relevance of Antarctic environmental forecasting services in decision-making processes by a diverse community of forecast users, the survey and focus-group discussions during the workshop will explore the following: (i) decision-making; (ii) information/data being consulted in the process of decision-making; (iii) Antarctic environmental forecasting services; and (iv) societal relevance and benefits.

This Antarctic Weather & Society workshop is part of a larger PPP initiative to facilitate the transition from science to service provision and will be supplemented by a series of similar workshops held in the Northern Hemisphere in 2021 and focused on the Arctic. The results from these deliberations will be shared at the YOPP Final Summit in Montréal, Canada, in 2022.

## ***10.*** *Conclusions*

The summer predictive skill for Antarctic latitudes is significantly poorer than that for the Arctic (Figure 5), confirming the need for the YOPP-SH effort. With no indigenous population, environmental forecasts primarily support operational and scientific activities, and surface wind forecasts are of most value (Figure 14). Observing system experiments have had limited initial success in improving predictions of surface winds (Figure 10), perhaps indicating that model boundary layer schemes need focused attention via YOPPsiteMIP.  As outlined here, efforts by the Antarctic research community have led to a successful YOPP-SH in the summer, and attention is now turning to the colder part of the year anticipating year-round research in the Antarctic.

**Acknowledgments**

This is a contribution to the Year of Polar Prediction (YOPP), a flagship activity of the Polar Prediction Project (PPP), initiated by the World Weather Research Programme (WWRP) of the World Meteorological Organisation (WMO). We acknowledge the WMO WWRP for its role in coordinating this international research activity. The Scientific Committee on Antarctic Research (SCAR) via the standing Physical Sciences Group has been an enthusiastic participant in YOPP-SH from the beginning and funded the publication of this manuscript that is contribution 1596 of Byrd Polar & Climate Research Center. DHB, JP, and KM are supported by NSF PLR 1823135. MAL is supported by NSF PLR 1543305. JI is supported by a JSPS Grants-in-Aid for Scientific Research (KAKENHI) 18H05053. FM is a F.R.S.-FNRS Research Fellow. Also FM was a member of the Southern Ocean Regional Panel (SORP) during the preparation of this manuscript, and SORP thanks its co-sponsors: Climate and Ocean Variability, Predictability and Change (CLIVAR) and Climate and Cryosphere (CliC) core programs of the World Climate Research Programme in conjunction with SCAR. Logistical support for YOPP-SH activities at French Antarctic stations was provided by the French Polar Institute IPEV through project CALVA 1013. For AR measurements made at Escudero Station, the authors are grateful to the Chilean Antarctic Institute (INACH) for logistical support and to Edgardo Sepulveda, Jose Jorquerra, and Braulio Valdevenito for their efforts supporting and maintaining the research platform. Nicolas Dettling and Edgardo Sepulveda helped with AR data collection. RC and PMR acknowledge funding from Fondecyt Regular 1161460. PMR also acknowledges funding from NSF PLR 1543236 and from NorthWest Research Associates. IVG thanks FCT/MCTES for the financial support to CESAM (UID/ AMB/50017/2019) through national funds. Special observations of KOPRI-SH at the King Sejong station were supported by PE19010 from the Korea Polar Research Institute. PS and HK were logistically supported by University of Magallanes, Punta Arenas, and received financial support through the European Research Infrastructure for the observation of Aerosol, Clouds and Trace Gases ACTRIS under grant agreement no. 654109 and 739530 from the European Union's Horizon 2020 research and innovation program as well through project 408008112 from the German Science Foundation (DFG). CAPIRE-YOPP was funded by contributions of Milano-Bicocca University and PNRA, and field activities in Antarctica were supported by ENEA scientific personnel operating the Meteo-Climatological Observatory. In Italy CAPIRE-YOPP was a success due to essential cooperation with the Meteo Service of the Italian Air Force. Finally, we appreciate the constructive comments from the two anonymous reviewers.

## References


Barker, D.M., and Co-Authors, 2012: The Weather Research and Forecasting Model's community variational/ensemble data assimilation system: WRFDA. *Bull Amer. Meteor. Soc.*, **93**, 831–843.

Bozkurt, D., R. Rondanelli, J.C. Marin, and R. Garreaud, 2018: Foehn event triggered by an atmospheric river underlies record-setting temperature along continental Antarctica. *J. Geophys. Res. Atmos.*, **123**, 3871– 3892. https://doi.org/10.1002/2017JD027796.

Dawson, J., W. Hoke, M.A.J. Lamers, D. Liggett, G. Ljubicic, B. Mills, E. Stewart, and R. Thoman, 2017: Navigating Weather, Water, Ice and Climate Information for Safe Polar Mobilities, WWRP/PPP No. 5, World Meteorological Organization.

Day, J., I. Sandu, L. Magnusson, M. J. RodwelI, H. Lawrence, N. Bormann, and T. Jung, 2020: Increased Arctic influence on the mid-latitude flow during Scandinavian blocking episodes. *Quart. J. Roy. Meteor. Soc.*, in press, https://doi.org/10.1002/qj.3673.

Enomoto T., A. Kuwano-Yoshida, N. Komori, and W. Ohfuchi, 2008: Description of AFES2: Improvements for high-resolution and coupled simulations. In *High Resolution Numerical Modelling of the Atmosphere and Ocean*, edited by K. Hamilton and W. Ohfuchi, chap. 5, pp. 77–97, Springer, New York.

Enomoto, T., T. Miyoshi, Q. Moteki, J. Inoue, M. Hattori, A. Kuwano-Yoshida, N. Komori, and S. Yamane, 2013: Observing-system research and ensemble data assimilation at JAMSTEC. In *Data Assimilation for Atmospheric, Oceanic and Hydrologic Applications (Vol. II)*, edited by S. K. Park and L. Xu, chap. 21, pp. 509–526, Springer, Berlin.

Goessling, H.F., S. Tietsche, J.J. Day, E. Hawkins, and T. Jung, 2016: Predictability of the Arctic sea ice edge. *Geophys. Res. Lett.*, **43**, 1642–1650. https://doi.org/10.1002/2015GL067232.

Gonzalez, S., M. Bañon, J.V. Albero, R. Larramendi, H. Moreno, F. Vasallo, P. Sanz, A. Quesada, and A. Justel, 2019: Weather observations of remote polar areas using an AWS onboard a unique zero-emissions polar vehicle. *Bull. Amer. Meteor. Soc*., **100**, 1891–1895, doi: 10.1175/BAMS-D-19-0110.1.

Gorodetskaya, I. V., M. Tsukernik, K. Claes, M.F. Ralph, W.D. Neff, and N.P. M. Van Lipzig, 2014: The role of atmospheric rivers in anomalous snow accumulation in East Antarctica, *Geophys. Res. Lett.*, 41, 6199– 6206, doi:10.1002/2014GL060881.

Gorodetskaya, I.V., T. Silva, H. Schmithüsen, and N. Hirasawa, 2020: Atmospheric river signatures in radiosonde profiles and reanalyses at the Dronning Maud Land coast, East Antarctica. *Adv. Atmos. Sci.* **37,** 455–476. https://doi.org/10.1007/s00376-020-9221-8.

Holland, M.M., E. Blanchard-Wrigglesworth, J. Kay, and S. Vavrus, 2013: Initial-value predictability of Antarctic sea ice in the Community Climate System Model 3. *Geophys. Res. Lett.,* **40**, 2121–2124, https://doi.org/10.1002/grl.50410.

Holland, M.M., L. Landrum, M. Raphael, and S. Stammerjohn, 2017: Springtime winds drive Ross Sea ice variability and change in the following autumn. *Nat. Commun.*, **8**, 731. https://doi.org/10.1038/s41467-017-00820-0.

Hunt, B. R., E. J. Kostelich, and I. Szunyogh, 2007: Efficient data assimilation for spatiotemporal chaos: A local ensemble transform Kalman filter. *Physica D: Nonlinear Phenomena*, **230**, 112–126.

Inoue, J., A. Yamazaki, J. Ono, K. Dethloff, M. Maturilli, R. Neuber, P. Edwards, and H. Yamaguchi, 2015: Additional Arctic observations improve weather and sea-ice forecasts for the Northern Sea Route. *Sci. Rep.*, **5**, 16868.

Jung, T., and Coauthors, 2016: Advancing polar prediction capabilities on daily to seasonal time scales. *Bull. Amer. Meteor. Soc.*, **97**, 1631–1647. doi:10.1175/BAMS-D-14-00246.1.

Marchi, S., T. Fichefet, H. Goosse, V. Zunz, S. Tietsche, J.J. Day, and E. Hawkins, 2019: Reemergence of Antarctic sea ice predictability and its link to deep ocean mixing in global climate models. *Clim. Dyn.,* **52**, 2775–2797, https://doi.org/10.1007/s00382-018-4292-2.

Massonnet, F., P. Reid, C.M. Bitz, J.C. Fyfe, and W.R. Hobbs, 2018: Assessment of February 2018 sea-ice forecasts for the Southern Ocean.

Massonnet, F., P. Reid, C.M. Bitz, J.C. Fyfe, and W.R. Hobbs, 2019: Assessment of summer 2018-2019 sea-ice forecasts for the Southern Ocean.

Meehl, G.A., J.M Arblaster, C.T.Y. Chung, M.M. Holland, A. DuVivier, L. Thompson, D. Yang, and C.M. Bitz, 2019: Sustained ocean changes contributed to sudden Antarctic sea ice retreat in late 2016. *Nat. Commun.,* **10**, 14, https://doi.org/10.1038/s41467-018-07865-9.

Miyoshi, T., and S. Yamane, 2007: Local ensemble transform Kalman filtering with an AGCM at a 159/L48 resolution. *Mon. Wea. Rev.*, **135**, 3841–3861.

Morss, R. E., J.K. Lazo, B.G. Brown, H.E. Brooks, P.T. Ganderton, and B.N. Mills, 2008: Societal and economic research and applications for weather forecasts: Priorities for the North American THORPEX Program. *Bull. Amer. Meteor. Soc.*, **89**(3), 335-346, doi:10.1175/bams-89-3-335.

Ohfuchi, W., H. Nakamura, M. K. Yoshioka, T. Enomoto, K. Tanaka, X. Peng, S. Yamane, T. Nishimura, Y. Kurihara, and K. Ninomiya, 2004: 10-km mesh mesoscale resolving simulations of the global atmosphere on the Earth Simulator: Preliminary outcomes of AFES (AGCM for the Earth Simulator). *J. Earth Simulator, **1**, 8–34.*

Ordoñez, A.C., C.M. Bitz, and E. Blanchard-Wrigglesworth, 2018: Processes controlling Arctic and Antarctic sea ice predictability in the Community Earth System Model. *J. Clim.,* **31**, 9771–9786, https://doi.org/10.1175/JCLI-D-18-0348.1.

Pailleux, J., J.-F. Geleyn, R. El Khatib, C. Fischer, M. Hamrud, J.-N. Thépaut, F. Rabier, E. Andersson, D. Salmond, D. Burridge, A. Simmons, and P. Courtier, 2015: Les 25 ans du système de prévision numérique du temps IFS/Arpège. *La Météorologie*, **89**, 18-27, doi:10.4267/2042/56594

Parkinson, C.L., 2019: A 40-y record reveals gradual Antarctic sea ice increases followed by decreases at rates far exceeding the rates seen in the Arctic. *Proc. Natl. Acad. Sci.*,**116**, 14414–14423, https://doi.org/10.1073/pnas.1906556116.

Powers, J.G., K.W. Manning, D.H. Bromwich, J.J. Cassano, and A.M. Cayette, 2012: A decade of Antarctic science support through AMPS. *Bull. Amer. Meteor. Soc.*, **93**, 1699–1712.

Sato, K., J. Inoue, A. Yamazaki, J.-H. Kim, M. Maturilli, K. Dethloff, S. R. Hudson, and M. A. Granskog, 2017: Improved forecasts of winter weather extremes over midlatitudes with extra Arctic observations. *J. Geophys. Res.*, **122**, 775– 787.

Sato, K., J. Inoue, A. Yamazaki, J.-H. Kim, A. Makshtas, V. Kustov, M. Maturilli, and K. Dethloff, 2018a: Impact on predictability of tropical and mid-latitude cyclones by extra Arctic observations. *Sci. Rep.*, **8**, 12104.

Sato, K., J. Inoue, S. P. Alexander, G. McFarquhar, and A. Yamazaki, 2018b: Improved reanalysis and prediction of atmospheric fields over the Southern Ocean using campaign-based radiosonde observations. *Geophys. Res. Lett.*, **45**, 11,406 – 11,413.

Sato, K., J. Inoue, A. Yamazaki, N. Hirasawa, K. Sugiura, and K. Yamada, 2020: Antarctic radiosonde observations reduce uncertainties and errors in reanalyses and forecasts over the Southern Ocean: an extreme cyclone case. *Adv. Atm. Sci.*, **37**, 1–9.

Schlosser, E., F.A. Haumann, and M.N. Raphael, 2018: Atmospheric influences on the anomalous 2016 Antarctic sea ice decay. *The Cryosphere*, **12**, 1103–1119, https://doi.org/10.5194/tc-12-1103-2018.

Skamarock, W. C., J. B. Klemp, J. Dudhia, D. O. Gill, Z. Liu, J. Berner, W. Wang, J. G. Powers, M. G. Duda, D. M. Barker, and X.-Y. Huang, 2019: A description of the Advanced Research WRF Version 4. NCAR Tech. Note, NCAR/TN-556+STR, 145 pp.

Stuecker, M.F., C.M Bitz, and K.C. Armour, 2017: Conditions leading to the unprecedented low Antarctic sea ice extent during the 2016 austral spring season. *Geophys. Res. Lett.,* **44**, 9008–9019, https://doi.org/10.1002/2017GL074691.

Wang, X., D. M. Barker, C. Snyder, and T. M. Hamill, 2008: A hybrid ETKF–3DVAR data assimilation scheme for the WRF model. Part I: Observing system simulation experiment. *Mon. Wea. Rev.*, **136**, 5116–5131.

Wang, Z., J. Turner, Y. Wu, and C. Liu, 2019: Rapid decline of total Antarctic sea ice extent during 2014–16 controlled by wind-driven sea ice drift. *J. Clim.,* **32**, 5381–5395, https://doi.org/10.1175/JCLI-D-18-0635.1.

Werner, K., 2017: Communication in an international WMO Project: Successfully linking between internal and external stakeholders for the Polar Prediction Project (in German). Masters Thesis, Technical University Berlin, Berlin, 94 pp.

Wille, J., V. Favier, A. Dufour, I. V. Gorodetskaya, J. Turner, C. Agosta, and F. Codron, 2019: West Antarctic surface melt triggered by atmospheric rivers. *Nat. Geosci.* **12,** 911–916, doi:10.1038/s41561-019-0460-1.

WMO-485: World Meteorological Organization “Manual on the Global Data processing and forecasting System” Published by WMO in 2017 and updated in 2018, available at https://library.wmo.int.

Yamazaki, A., J. Inoue, K. Dethloff, M. Maturilli, and G. König-Langlo, 2015: Impact of radiosonde observations on forecasting summertime Arctic cyclone formation. *J. Geophys. Res. Atmos.*, **120**, 3249–3273.

YOPP Implementation Plan, version 3, available at https://www.polarprediction.net/about/implementation-and-science-plans/.

Zampieri, L., H.F. Goessling, and T. Jung, 2019. Predictability of Antarctic sea ice edge on subseasonal time scales. *Geophys. Res. Lett.*, **46**, 9719–9727, https://doi.org/10.1029/2019GL084096.

**Figure Captions**

**Figure 1.** Count of additional radiosondes launched during the YOPP-SH SOP by land location and by ship (ship symbols plotted at representative locations). "King George Island" combines the soundings from Escudero and King Sejong stations. "Terra Nova Bay" merges the efforts of Mario Zucchelli and Jang Bogo stations. The extra radiosondes add to the routine launches from Rothera, Halley, Neumayer, Novolazarevskaya, Syowa, Mawson, Davis, Mirny, Casey, Dumont D'Urville, Macquarie Island, Mario Zucchelli, Dome C (AKA Concordia), McMurdo, and South Pole. McMurdo and South Pole each had two routine soundings per day but nothing in addition.

**Figure 2.** A map of all known Antarctic Automatic Weather Stations (AWS) sites operating in 2019.

**Figure 3**. Overview of drifting buoys active at the start of the YOPP-SH SOP during November 2018. Those in yellow only report surface temperature to the GTS while those in green also report surface pressure. Purple buoys close to Antarctica were some of those supplied by the Alfred Wegener Institute as outlined in detail in Figure 4. Drift tracks show the hourly locations during November 2018 with the dots denoting the position at the end of the month. Notice the very limited coverage south of about 60°S primarily due to sea-ice cover.

**Figure 4.** Overview of drift trajectories of all buoys originating in the Weddell Sea that were active during the YOPP-SH SOP. Black lines show the entire drift trajectories with the black dot marking the end of the respective buoy drift. The actual drift path of each buoy during the SOP is colored respectively. The buoy names are composed of the year of deployment, buoy types and a consecutive number. Buoy types are: Ice Mass Balance Buoys (M), Snow Buoys (S), Surface Velocity Profilers (P) and Radiation Stations (R).

**Figure 5**. Anomaly correlation coefficient of operational global models for the 500-hPa geopotential height field for (top) Antarctica (solid lines) versus the extratropical Southern Hemisphere (dashed lines), and (bottom) of the Arctic (solid lines) versus the extratropical Northern Hemisphere (dashed lines), during the respective summers. Verification is against each model's own forecast. Notice the superior forecast performance for the Arctic shown by the larger anomaly correlation coefficients versus the Antarctic (solid colors). The Australian BOM SH performance (grey, top) is degraded during the SOP because of numerical instability over Antarctica. Subsequently, their new ACCESS-G model version has a forecast performance approaching that of the related UKMO.

**Figure 6**. The Canadian Global Model (ECCP-GDPS) surface air temperature bias evaluated for the raw model output (red lines), and for the model output adjusted to the station elevation by applying the standard-atmosphere WMO-recommended lapse rate (0.0065 K/m, gray lines), and the dry adiabatic lapse rate (0.0098K/m, blue lines). The dashed lines show the bias calculated excluding stations which differ in elevation more than 500m from the model-tile altitude.

**Figure 7.** RMSE differences between ARPEGE and ARPEGE-SH (blue means positive impact) for forecast and observed temperature during the YOPP-SH SOP as a function of forecast hour and pressure level for the domain 90˚S-20ºS. Left: against radiosondes. Right against the ERA5 global reanalysis. Iso-lines every 0.05K.

**Figure 8.** AMPS WRF forecast grids. Outer frame shows the 24-km WRF grid run for the forecast experiments and the data assimilation ensembles. Finer, regional nests (8 km, 2.67 km and 0.89 km) that are also run in AMPS also shown.

**Figure 9.** Sea level pressure (shaded, hPa, scale to right) and surface winds (vectors) from 48-hr SOP forecast (top left) and no-SOP forecast (top right) and from the ERA5 global reanalysis

(bottom), valid 00 UTC 18 January 2019. Coast of West Antarctica shown and Austin AWS marked.

**Figure 10.** Time series of surface pressure (hPa, top panel), 2-m temperature (°C, middle panel), and 10-m wind speed ($ms^{-1}$, bottom panel) for the Austin AWS site in West Antarctica from no-SOP run (blue), SOP run (red), ERA5 global reanalysis (green), and AWS observations (black). Location of Austin marked in Figure 8. Period shown is 12 UTC 16–20 January 2019, with model values taken from forecasts initialized at 00 UTC 16 January. Panel insets show correlation coefficients and average bias error (°C) for the period for each data source.

**Figure 11.** a) Integrated water vapor (IWV, shading) and mean sea level pressure (contours) on 6 December 2018, 18 UTC, when an atmospheric river was affecting both Punta Arenas and King George Island (KGI); b) temporal evolution of IWV and cloud liquid water path (LWP) at Punta Arenas and IWV at KGI during 4-7 December 2018; c) radiosonde vertical profiles at KGI during the peak of the AR: moisture transport (meridional (MTv), zonal (MTu) and total (MT)) (left panel), temperature (T) and RH with respect to ice (RHi) (center panel), and specific humidity (SH), wind speed (WS) and wind direction (WD) (right panel); d) downwelling broadband shortwave (SW) and longwave (LW) fluxes from measurements together with calculations for clear skies (Clear) at Escudero (KGI); e) accumulated rain (in mm, total accumulated over the period from 5 December 2018 12 UTC to 8 Dec 2018 12 UTC) for the data assimilation experiment with Polar-WRF model (left) and wind speeds (right; top) and rainfall rates (right; bottom) for ERA5 global reanalysis, the control (CTL) and data assimilation (DA) model runs, and observations at an Automatic Meteorological Observation Station (AMOS) at King Sejong (KGI).

**Figure 12.** Integrated Ice Edge Error (IIEE; Goessling et al., 2016), a measure of spatial agreement of forecasted and observed sea-ice concentration, for dynamical model (blue) and statistical (orange) contributions participating in the austral summer 2018-2019 SIPN South coordinated forecast. The common reference verification product is NSIDC-0081 (https://nsidc.org/data/nsidc-0081). Low values indicate high skill, the shadings (when available) indicate the ensemble range for a given forecasting system. The black line is the IIEE for an alternative observation product and is meant to represent uncertainty in the verification product itself.

**Figure 13.** The final CAPIRE-YOPP event at Milan, Italy with participation by students, teachers, and schools (top). The launching of an extra sounding from Dome Concordia supported by CAPIRE-YOPP (bottom). Attached to the balloon is one of the drawings by a winning student.

**Figure 14.** Usefulness of weather information items during deployment to the Antarctic and/or sub-Antarctic. Percent of participant responses to the question: "On a scale from 1 (not at all useful) to 10 (most useful), please assess how useful you find each of the following items when you are in the Antarctic and/or sub-Antarctic."

**Figure 15.** Overview of communication (online and social media) activities during the YOPP Special Observing Period in the Antarctic.

**Figure 16.** Elements of the YOPP Consolidation Phase (from YOPP Implementation Plan, version 3).


**Figure 1.** Count of additional radiosondes launched during the YOPP-SH SOP by land location and by ship (ship symbols plotted at representative locations). "King George Island" combines the soundings from Escudero and King Sejong stations. "Terra Nova Bay" merges the efforts of Mario Zucchelli and Jang Bogo stations. The extra radiosondes add to the routine launches from Rothera, Halley, Neumayer, Novolazarevskaya, Syowa, Mawson, Davis, Mirny, Casey, Dumont D'Urville, Macquarie Island, Mario Zucchelli, Dome C (AKA Concordia), McMurdo, and South Pole. McMurdo and South Pole each had two routine soundings per day but nothing in addition.

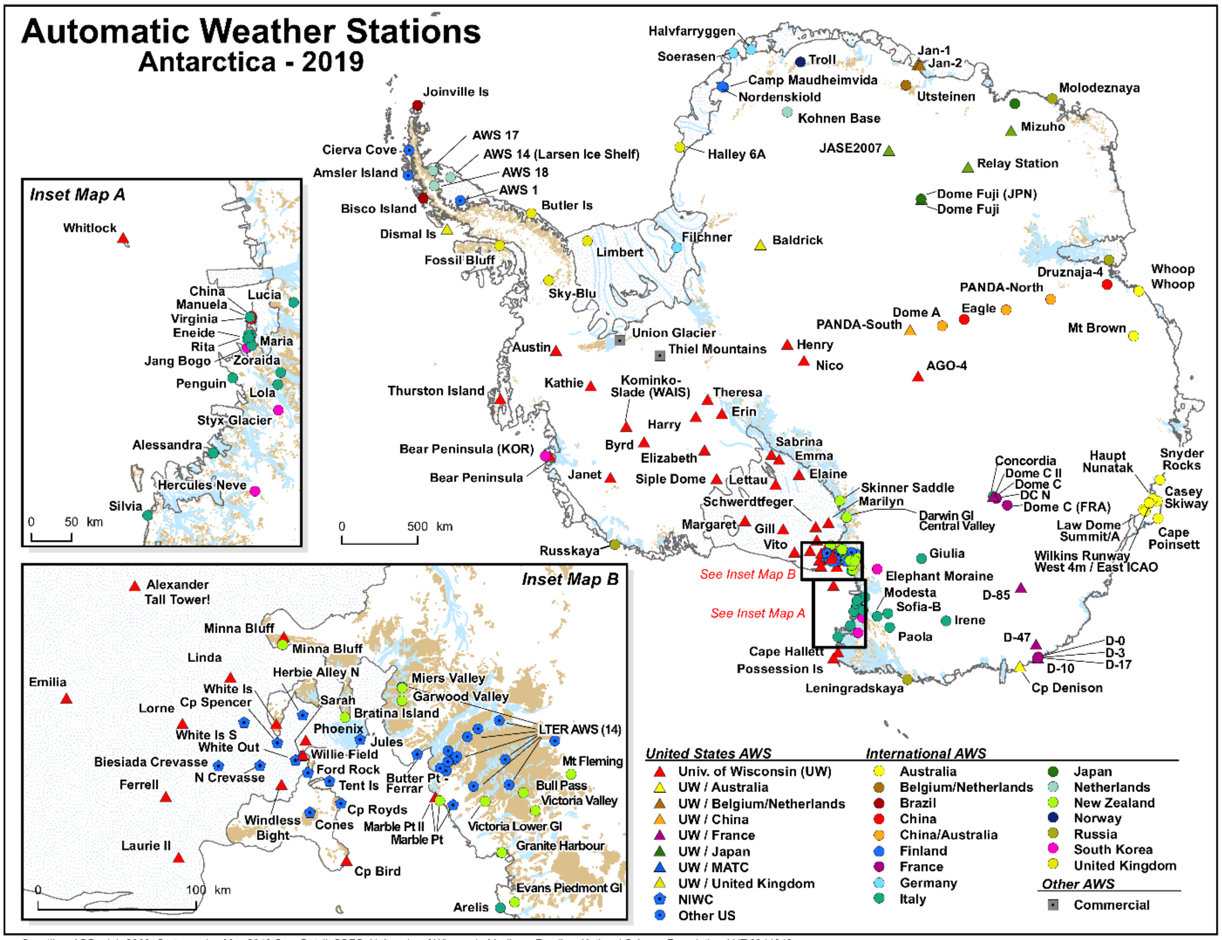


Coastline: ADD v4.1, 2003; Cartography: May 2019 Sam Batzli, SSEC, University of Wisconsin-Madison; Funding: National Science Foundation ANT-0944018

**Figure 2**. A map of all known Antarctic Automatic Weather Stations (AWS) sites operating in 2019.

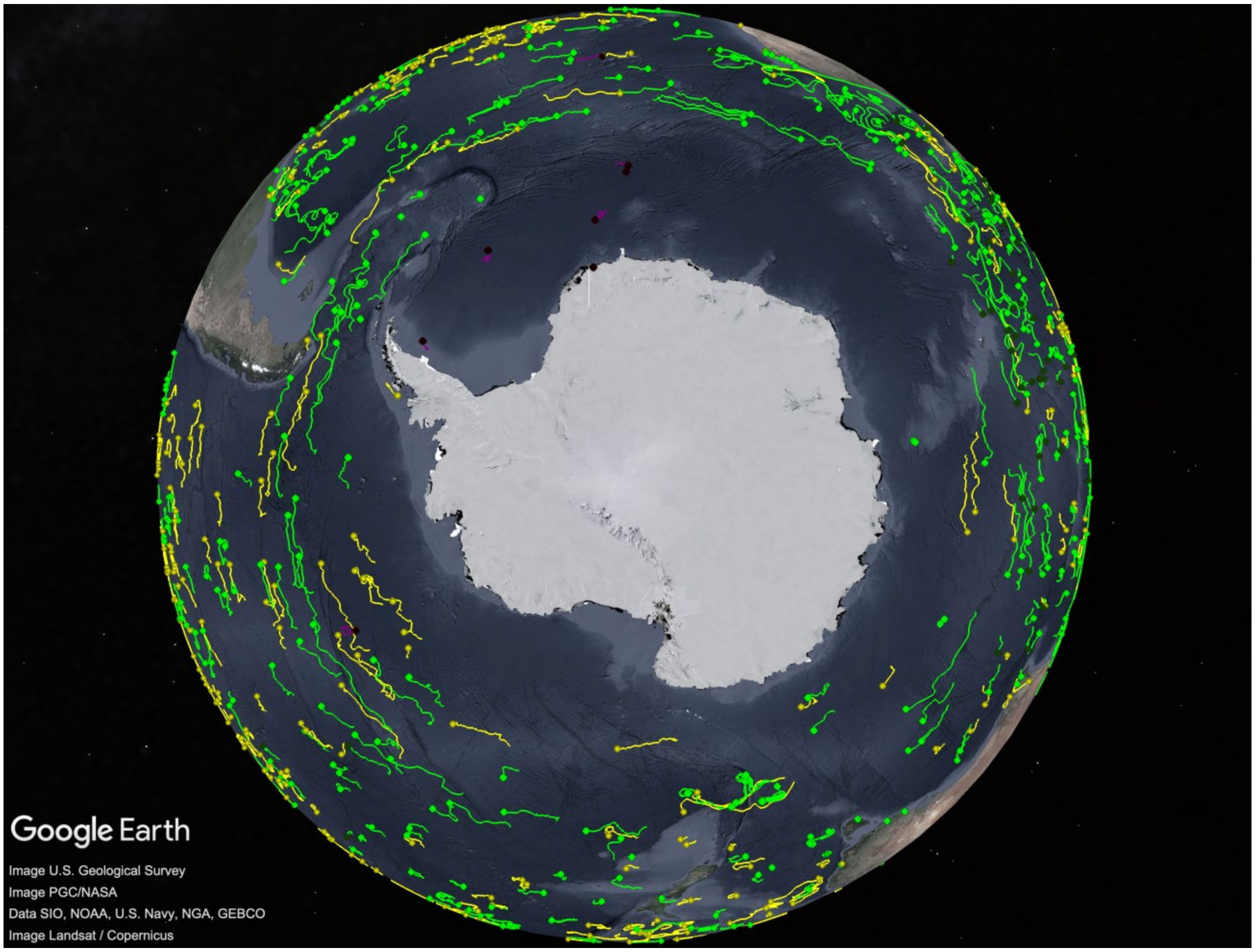


**Figure 3**. Overview of drifting buoys active at the start of the YOPP-SH SOP during November 2018. Those in yellow only report surface temperature to the GTS while those in green also report surface pressure. Purple buoys close to Antarctica were some of those supplied by the Alfred Wegener Institute as outlined in detail in Figure 4. Drift tracks show the hourly locations during November 2018 with the dots denoting the position at the end of the month. Notice the very limited coverage south of about 60°S primarily due to sea-ice cover.

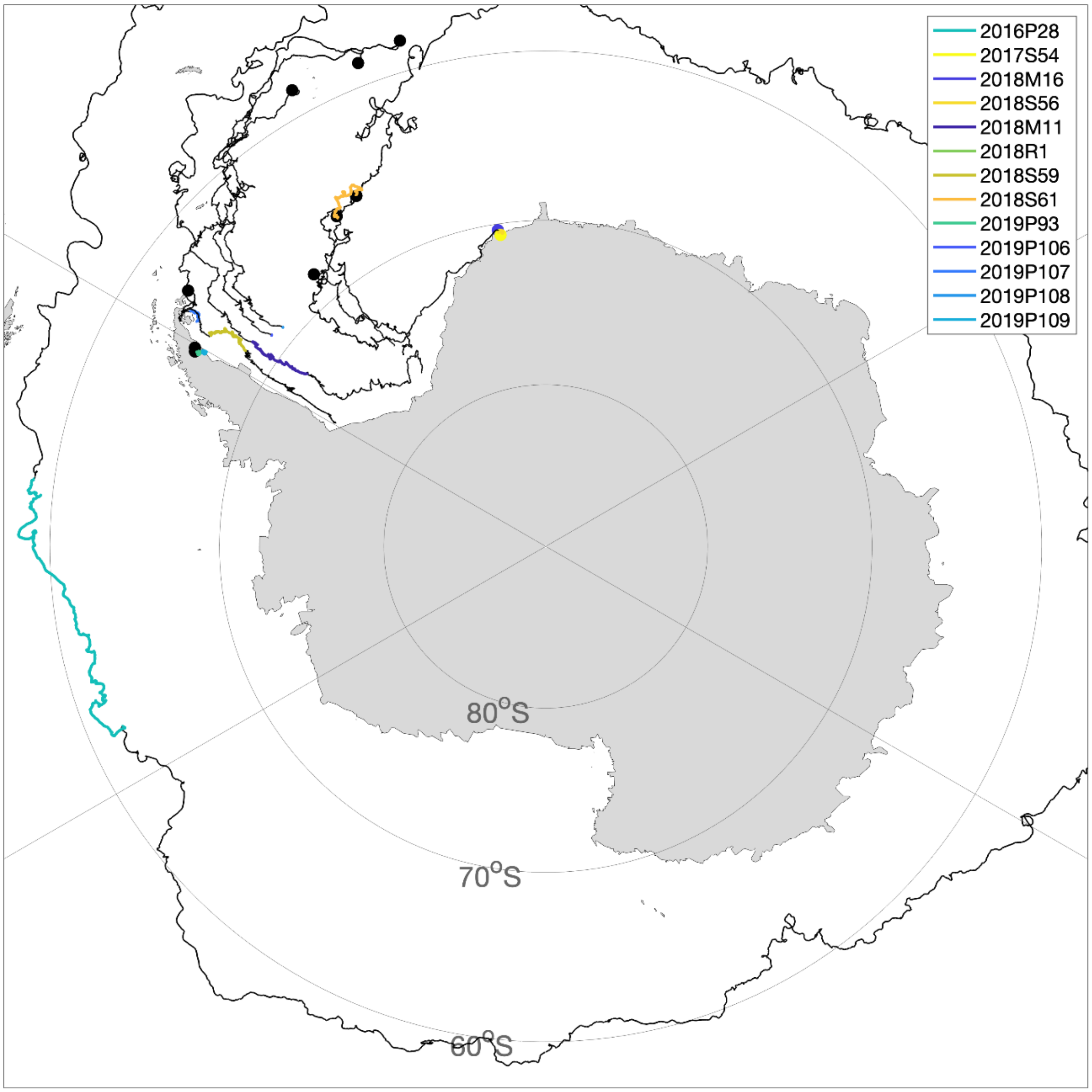


**Figure 4.** Overview of drift trajectories of all buoys originating in the Weddell Sea that were active during the YOPP-SH SOP. Black lines show the entire drift trajectories with the black dot marking the end of the respective buoy drift. The actual drift path of each buoy during the SOP is colored respectively. The buoy names are composed of the year of deployment, buoy types and a consecutive number. Buoy types are: Ice Mass Balance Buoys (M), Snow Buoys (S), Surface Velocity Profilers (P) and Radiation Stations (R).

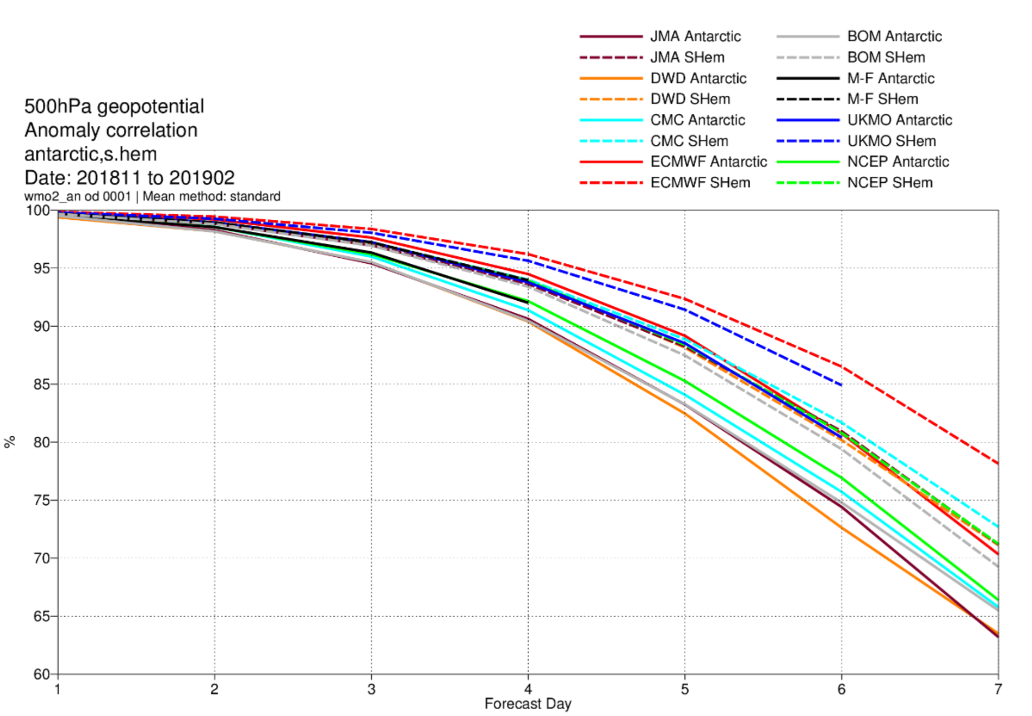
500hPa geopotential
Anomaly correlation
antarctic,s.hem
Date: 201811 to 201902
wmo2_an od 0001 | Mean method: standard
JMA Antarctic
JMA SHem
DWD Antarctic
DWD SHem
CMC Antarctic
CMC SHem
ECMWF Antarctic
ECMWF SHem
BOM Antarctic
BOM SHem
M-F Antarctic
M-F SHem
UKMO Antarctic
UKMO SHem
NCEP Antarctic
NCEP SHem
%
Forecast Day

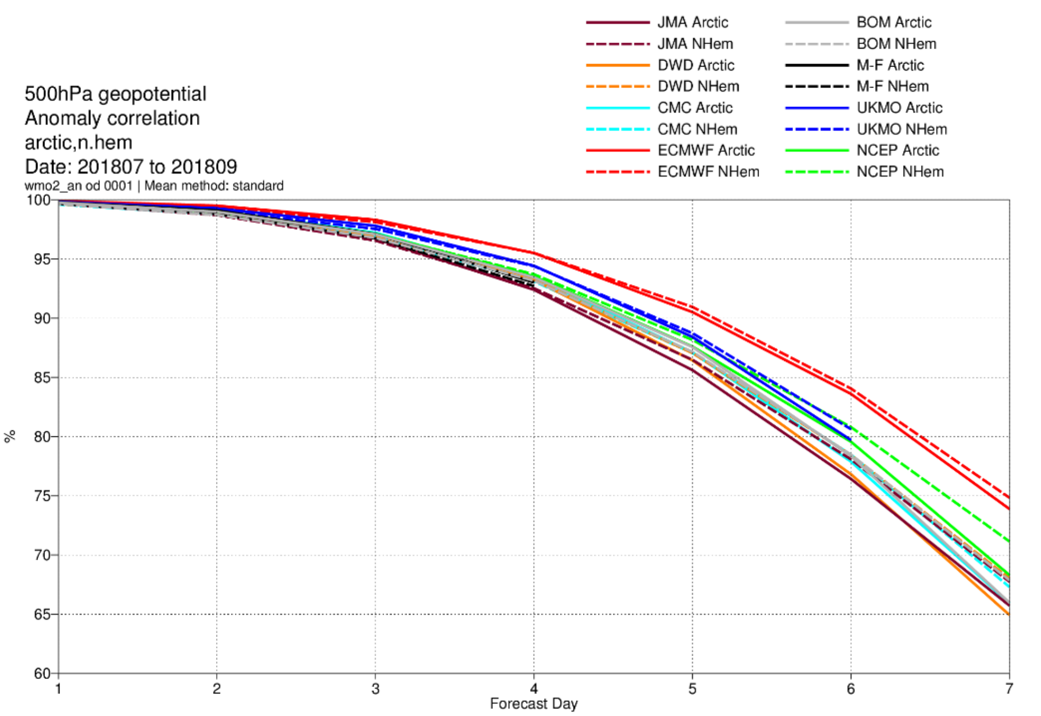
500hPa geopotential
Anomaly correlation
arctic,n.hem
Date: 201807 to 201809
wmo2_an od 0001 | Mean method: standard
JMA Arctic
JMA NHem
DWD Arctic
DWD NHem
CMC Arctic
CMC NHem
ECMWF Arctic
ECMWF NHem
BOM Arctic
BOM NHem
M-F Arctic
M-F NHem
UKMO Arctic
UKMO NHem
NCEP Arctic
NCEP NHem
%
Forecast Day

**Figure 5**. Anomaly correlation coefficient of operational global models for the 500-hPa geopotential height field for (top) Antarctica (solid lines) versus the extratropical Southern Hemisphere (dashed lines), and (bottom) of the Arctic (solid lines) versus the extratropical Northern Hemisphere (dashed lines), during the respective summers. Verification is against each model's own forecast. Notice the superior forecast performance for the Arctic shown by the larger anomaly correlation coefficients versus the Antarctic (solid colors). The Australian BOM SH performance (grey, top) is degraded during the SOP because of numerical instability over Antarctica. Subsequently, their new ACCESS-G model version has a forecast performance approaching that of the related UKMO.

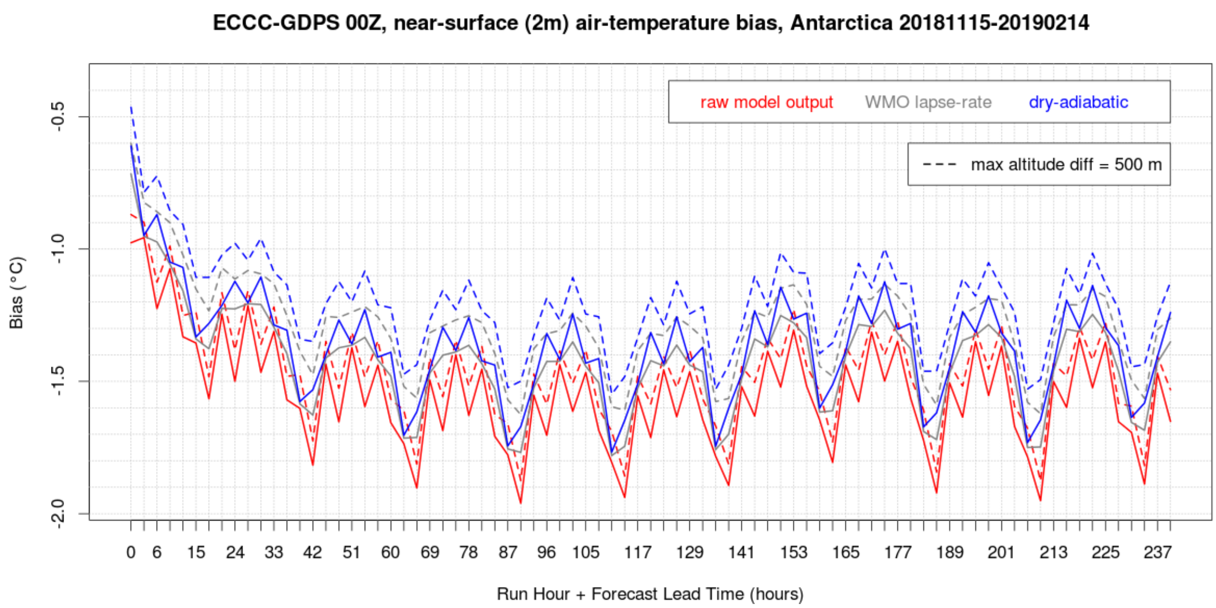


**Figure 6**. The Canadian Global Model (ECCP-GDPS) surface air temperature bias evaluated for the raw model output (red lines), and for the model output adjusted to the station elevation by applying the standard-atmosphere WMO-recommended lapse rate (0.0065 K/m, gray lines), and the dry adiabatic lapse rate (0.0098K/m, blue lines). The dashed lines show the bias calculated excluding stations which differ in elevation more than 500m from the model-tile altitude.

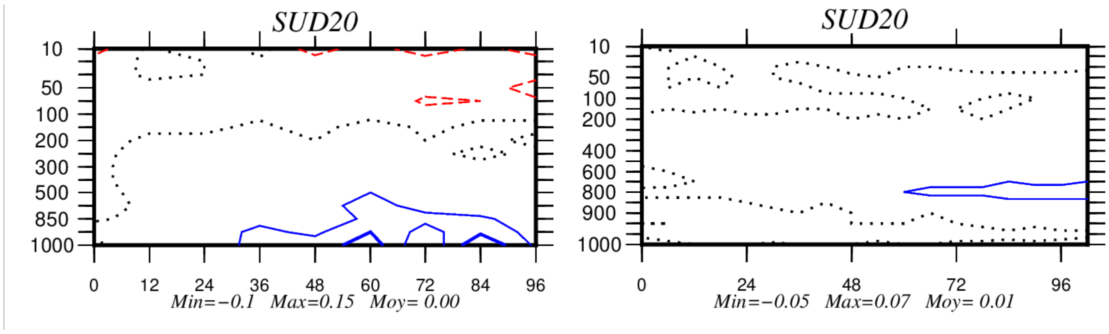


**Figure 7.** RMSE differences between ARPEGE and ARPEGE-SH (blue means positive impact) for forecast and observed temperature during the YOPP-SH SOP as a function of forecast hour and pressure level for the domain 90˚S-20ºS. Left: against radiosondes. Right against the ERA5 global reanalysis. Iso-lines every 0.05K.

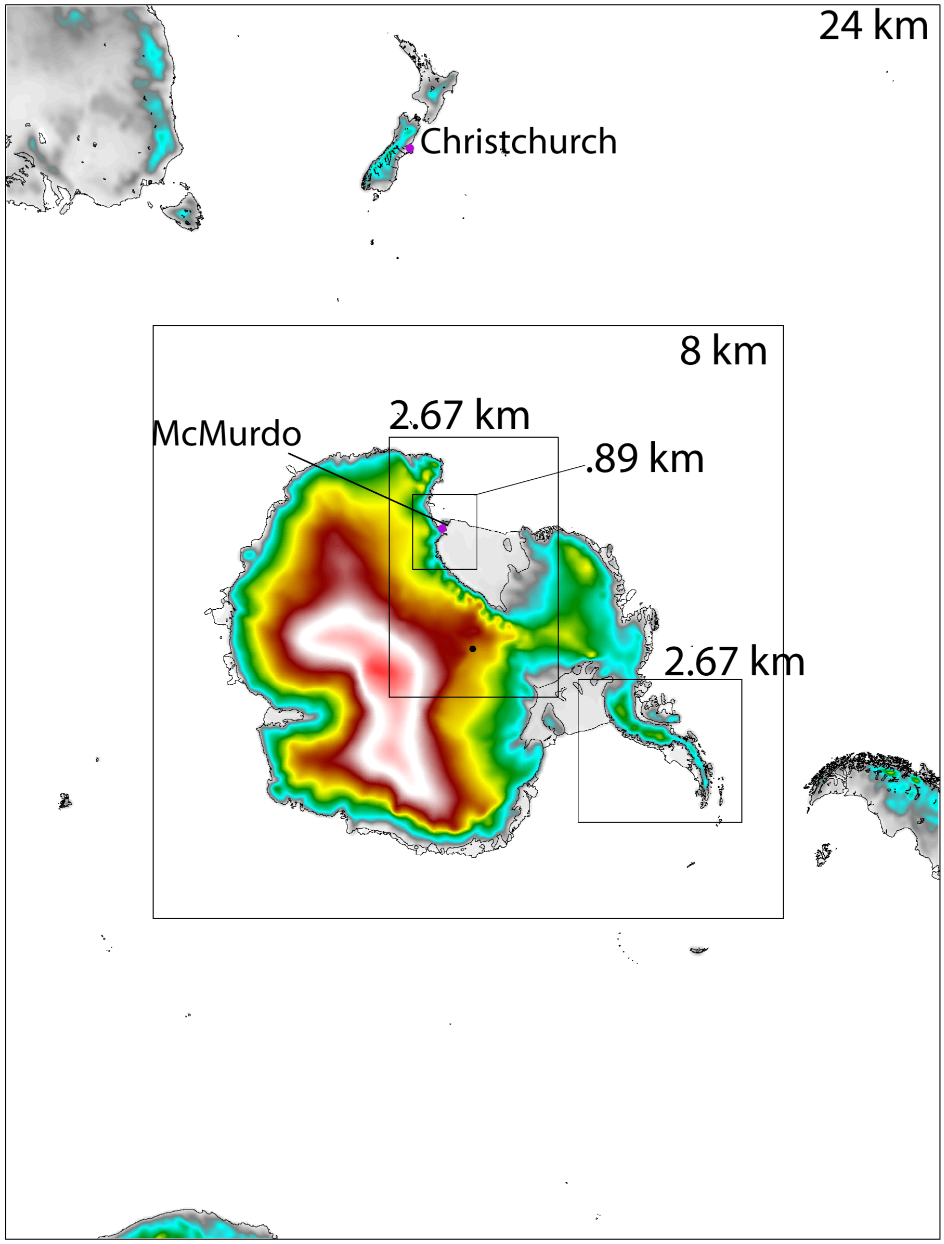


**Figure 8.** AMPS WRF forecast grids. Outer frame shows the 24-km WRF grid run for the forecast experiments and the data assimilation ensembles. Finer, regional nests (8 km, 2.67 km and 0.89 km) that are also run in AMPS also shown.

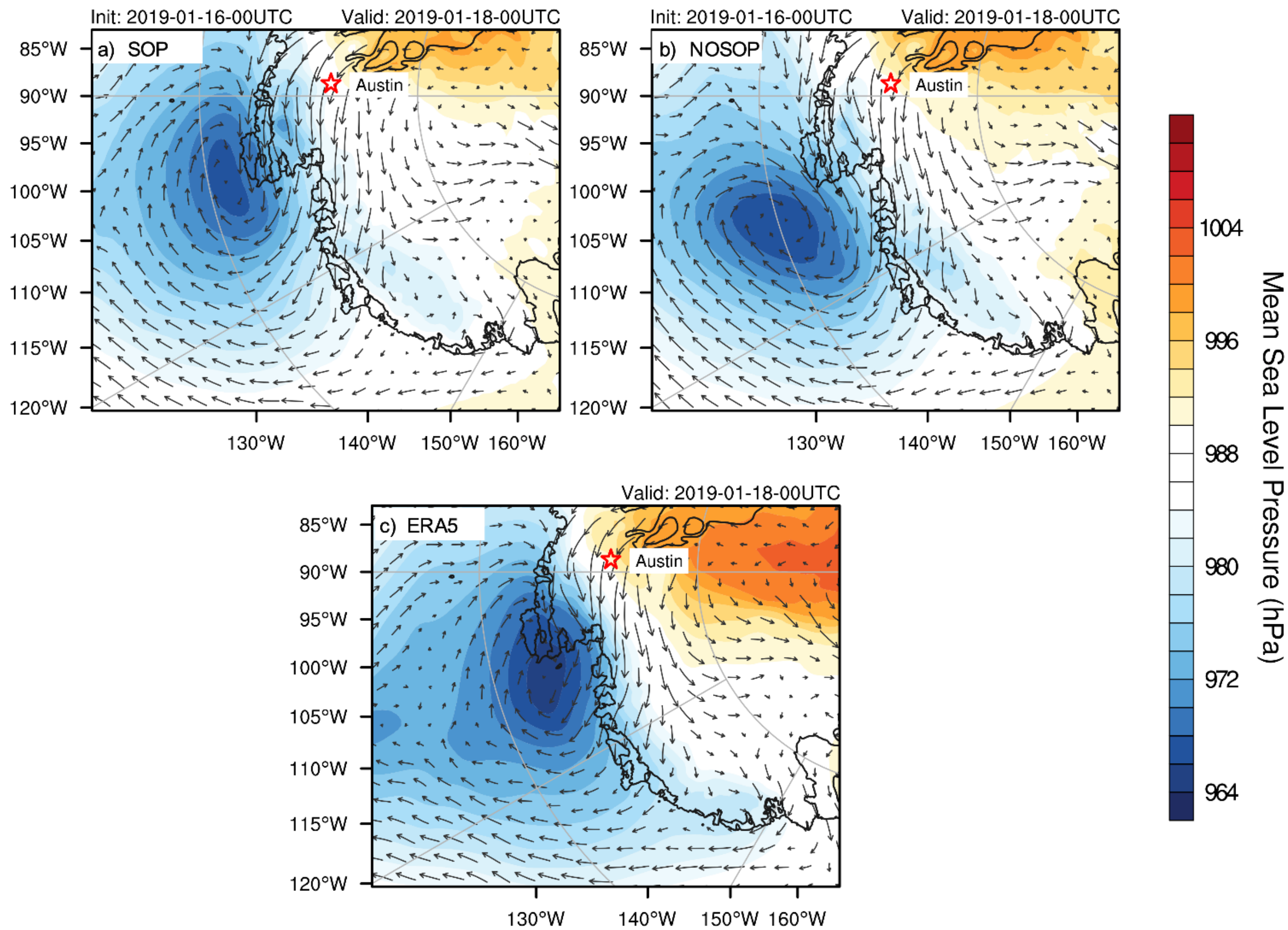


**Figure 9.** Sea level pressure (shaded, hPa, scale to right) and surface winds (vectors) from 48-hr SOP forecast (top left) and no-SOP forecast (top right) and from the ERA5 global reanalysis (bottom), valid 00 UTC 18 January 2019. Coast of West Antarctica shown and Austin AWS marked.

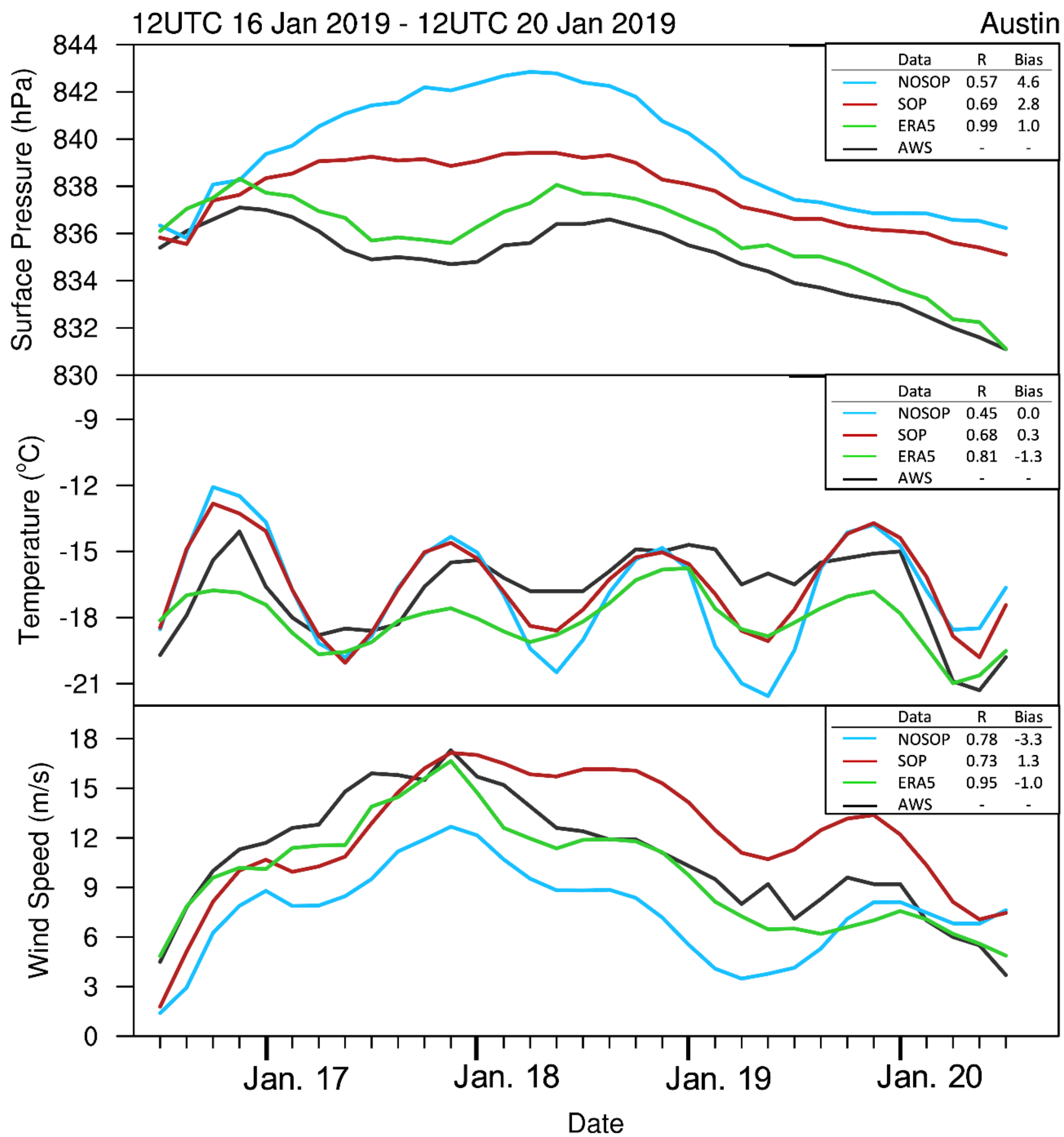


**Figure 10.** Time series of surface pressure (hPa, top panel), 2-m temperature (°C, middle panel), and 10-m wind speed (ms$^{-1}$, bottom panel) for the Austin AWS site in West Antarctica from no-SOP run (blue), SOP run (red), ERA5 global reanalysis (green), and AWS observations (black). Location of Austin marked in Figure 8. Period shown is 12 UTC 16–20 January 2019, with model values taken from forecasts initialized at 00 UTC 16 January. Panel insets show correlation coefficients and average bias error (°C) for the period for each data source.

a)

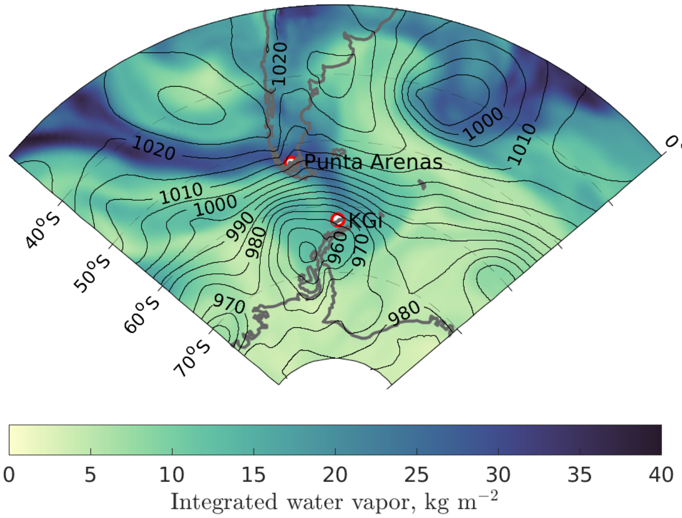
Punta Arenas
KGI
1020
1010
1000
990
980
970
960
40°S
50°S
60°S
70°S
0°
0 5 10 15 20 25 30 35 40
Integrated water vapor, kg m$^{-2}$

b)

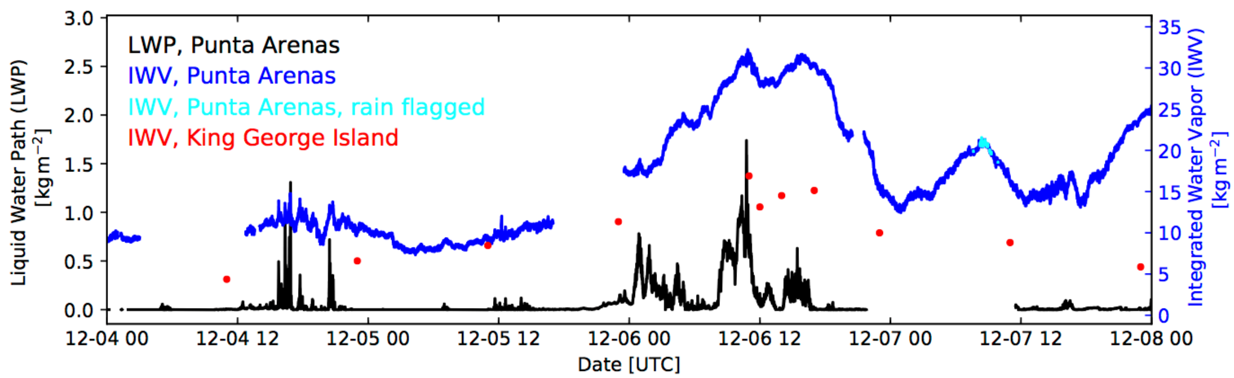
LWP, Punta Arenas
IWV, Punta Arenas
IWV, Punta Arenas, rain flagged
IWV, King George Island
Liquid Water Path (LWP) [kg m$^{-2}$]
Integrated Water Vapor (IWV) [kg m$^{-2}$]
Date [UTC]
12-04 00
12-04 12
12-05 00
12-05 12
12-06 00
12-06 12
12-07 00
12-07 12
12-08 00

c)

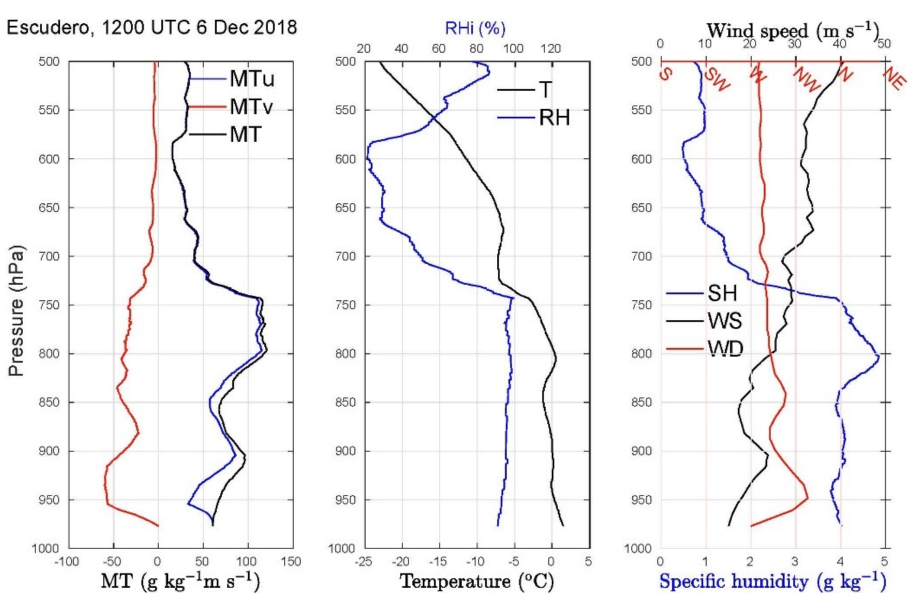
Escudero, 1200 UTC 6 Dec 2018
MTu
MTv
MT
Pressure (hPa)
MT (g kg$^{-1}$m s$^{-1}$)
RHi (%)
T
RH
Temperature (°C)
Wind speed (m s$^{-1}$)
S
SW
W
NW
N
NE
SH
WS
WD
Specific humidity (g kg$^{-1}$)

d)

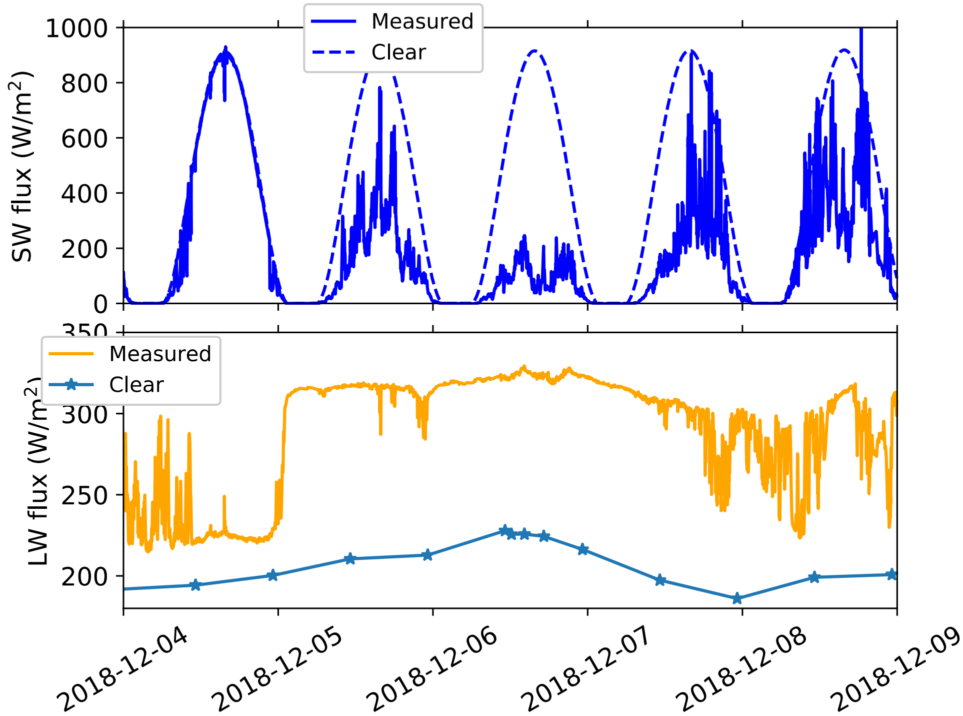


e)

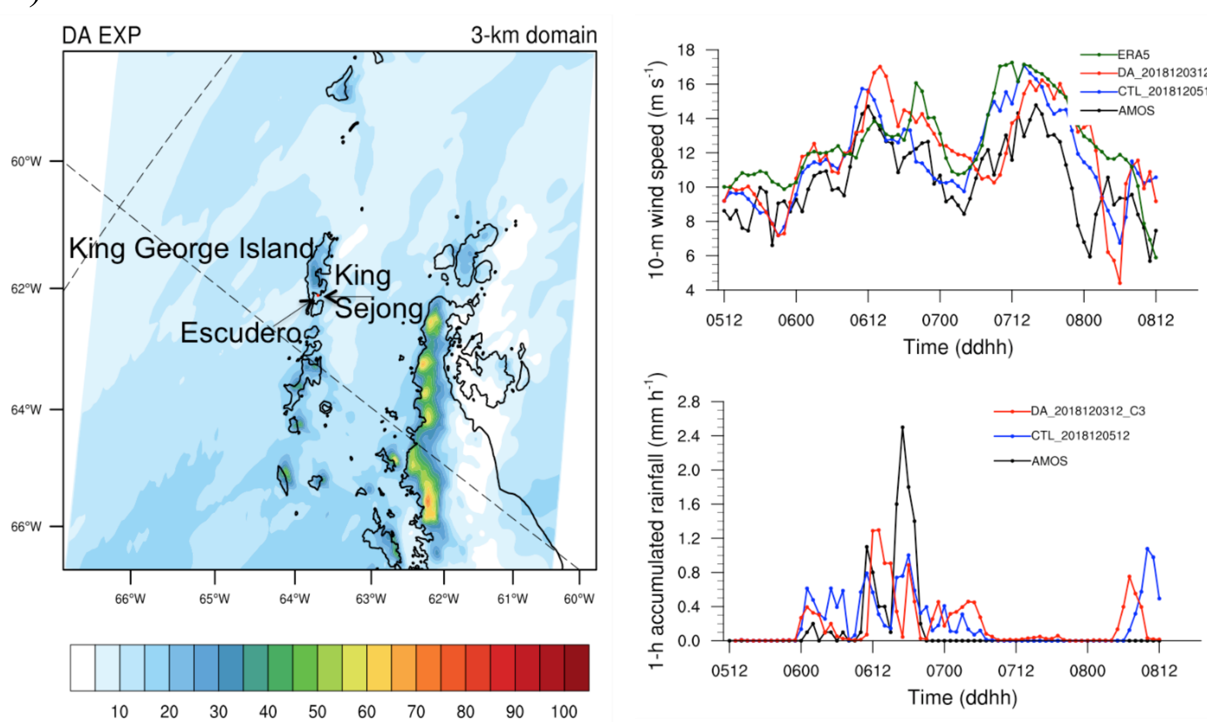


**Figure 11.** a) Integrated water vapor (IWV, shading) and mean sea level pressure (contours) on 6 December 2018, 18 UTC, when an atmospheric river was affecting both Punta Arenas and King

George Island (KGI); b) temporal evolution of IWV and cloud liquid water path (LWP) at Punta Arenas and IWV at KGI during 4-7 December 2018; c) radiosonde vertical profiles at KGI during the peak of the AR: moisture transport (meridional (MTv), zonal (MTu) and total (MT)) (left panel), temperature (T) and RH with respect to ice (RHi) (center panel), and specific humidity (SH), wind speed (WS) and wind direction (WD) (right panel); d) downwelling broadband shortwave (SW) and longwave (LW) fluxes from measurements together with calculations for clear skies (Clear) at Escudero (KGI); e) accumulated rain (in mm, total accumulated over the period from 5 December 2018 12 UTC to 8 Dec 2018 12 UTC) for the data assimilation experiment with Polar-WRF model (left) and wind speeds (right; top) and rainfall rates (right; bottom) for ERA5 global reanalysis, the control (CTL) and data assimilation (DA) model runs, and observations at an Automatic Meteorological Observation Station (AMOS) at King Sejong (KGI).

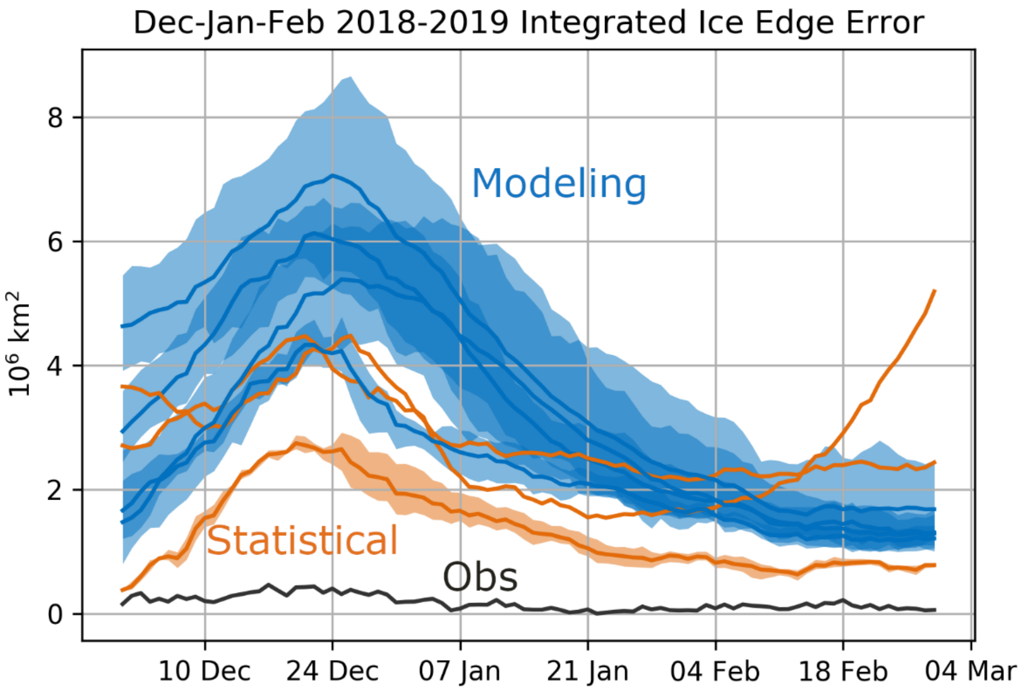


**Figure 12.** Integrated Ice Edge Error (IIEE; Goessling et al., 2016), a measure of spatial agreement of forecasted and observed sea-ice concentration, for dynamical model (blue) and statistical (orange) contributions participating in the austral summer 2018-2019 SIPN South coordinated forecast. The common reference verification product is NSIDC-0081 (https://nsidc.org/data/nsidc-0081). Low values indicate high skill, the shadings (when available) indicate the ensemble range for a given forecasting system. The black line is the IIEE for an alternative observation product and is meant to represent uncertainty in the verification product itself.

**Figure 13.** The final CAPIRE-YOPP event at Milan, Italy with participation by students, teachers, and schools (top). The launching of an extra sounding from Dome Concordia supported by CAPIRE-YOPP (bottom). Attached to the balloon is one of the drawings by a winning student.

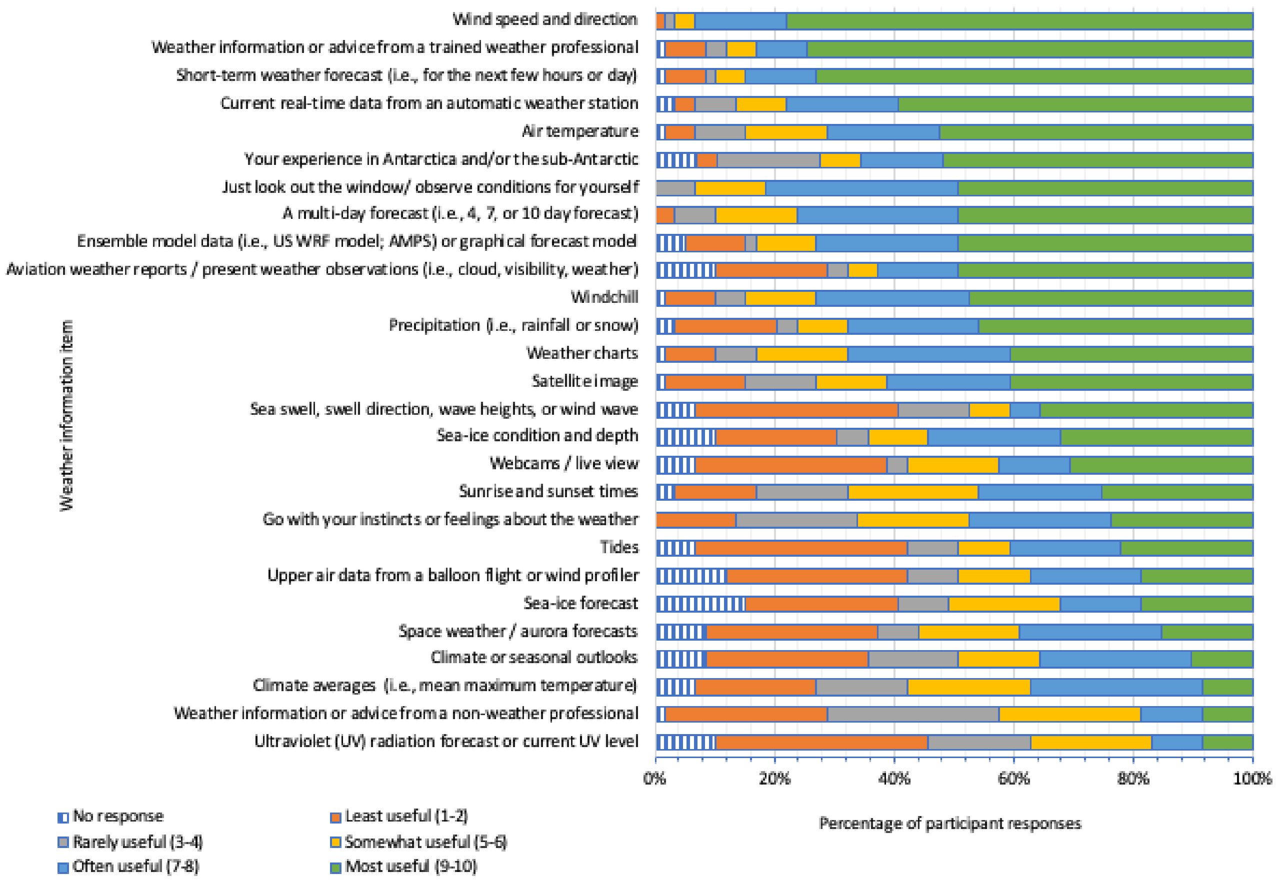


**Figure 14.** Usefulness of weather information items during deployment to the Antarctic and/or sub-Antarctic. Percent of participant responses to the question: "On a scale from 1 (not at all useful) to 10 (most useful), please assess how useful you find each of the following items when you are in the Antarctic and/or sub-Antarctic."

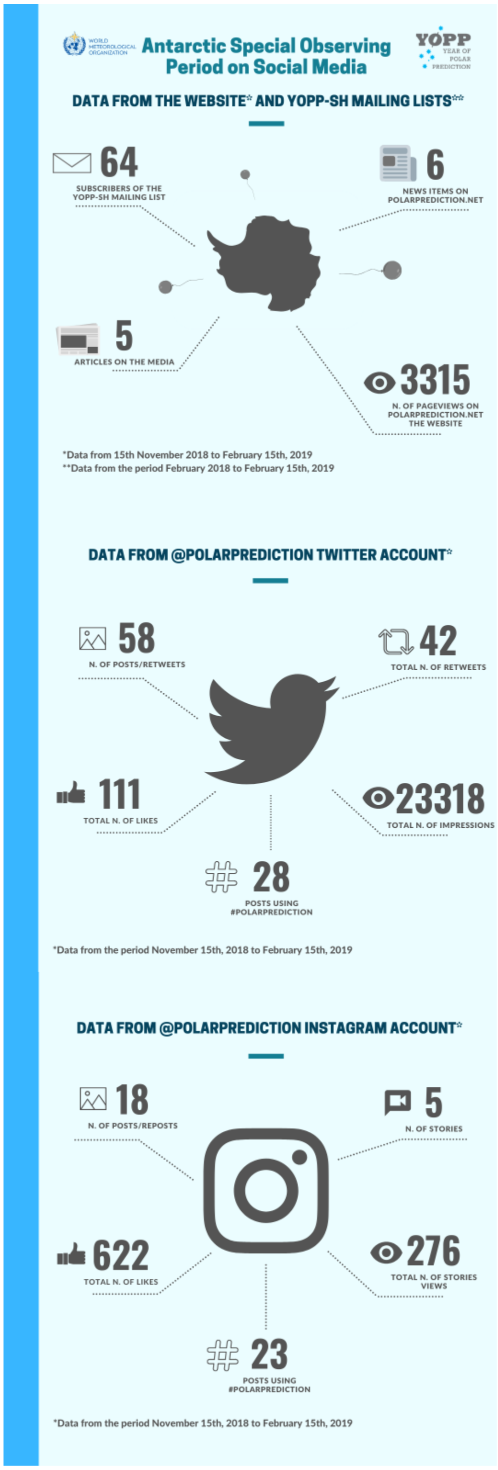


**Figure 15.** Overview of communication (online and social media) activities during the YOPP Special Observing Period in the Antarctic.

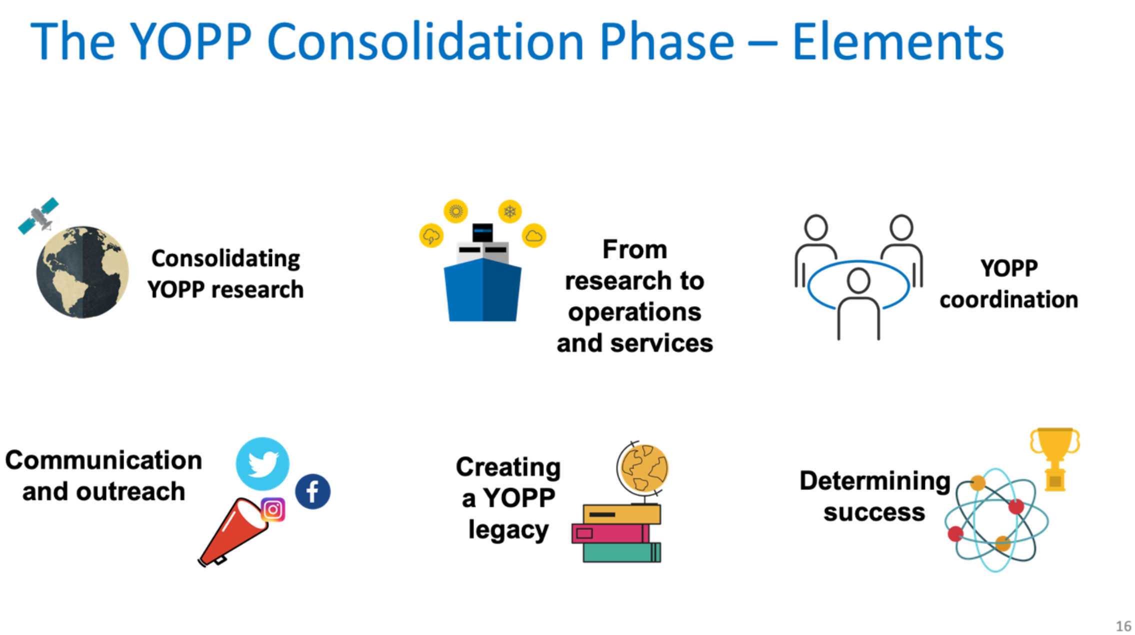


**Figure 16.** Elements of the YOPP Consolidation Phase (from YOPP Implementation Plan, version 3).